TITLE: Thermal Evolution of the Phlegraean Magmatic System

AUTHORS: Kenneth Wohletz[1], Lucia Civetta[2], and Giovanni Orsi[2]

[1]Los Alamos National Laboratory, Earth and Environmental Sciences Division, Los Alamos, NM 87545
[2]University of Naples Federico II, Department of Geophysics and Volcanology, Naples, Italy 80138
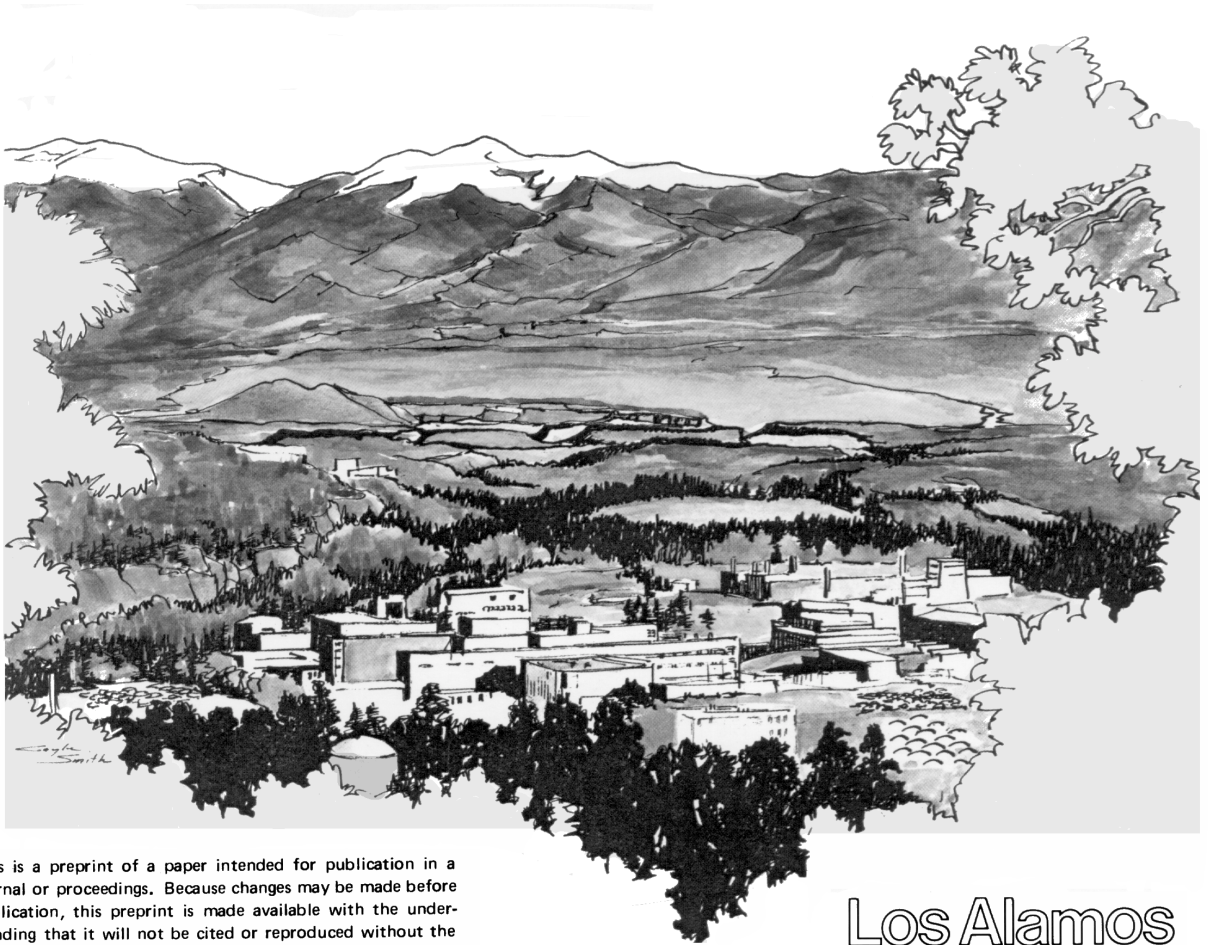
Los Alamos
Los Alamos National Laboratory
Los Alamos, New Mexico 87545

1

Thermal Evolution of the Phlegraean Magmatic System

Kenneth Wohletz

Earth and Environmental Sciences, Los Alamos National Laboratory, Los Alamos, NM USA

Lucia Civetta and Giovanni Orsi

Dipartimento di Geofisica e Vulcanologia, University of Napoli Federico II, Naples, Italy

Abstract

A series of 2-D conductive/convective numerical models show a rather limited range of possible magma chamber configurations that predict the present thermal regime at Campi Flegrei. These models are calculated by HEAT, which allows continuous adjustment of heterogeneous rock properties, magma injection/replenishment, and convective regimes. The basic test of each model is how well it reproduces the measured thermal gradients in boreholes at Licola, San Vito, and Mofete reported by AGIP in 1987. The initial and boundary conditions for each model consists of a general crustal structure determined by geology and geophysics and major magmatic events: (1) the 37 ka Campanian Ignimbrite; (2) smaller volume 37-16 ka eruptions; (3) the 12 ka Neapolitan Yellow Tuff; (3) recent magmatism (*e.g.*, Minopoli at ~10 ka and Monte Nuovo in 1538 AD). While magma chamber depth is well constrained, magma chamber diameter, shape, volume, and peripheral convective regimes are poorly known. Magma chamber volumes between 200 and 2000 km^3 have been investigated with cylindrical, conical (funnel-shaped), and spheroidal shapes. For all reasonable models, a convective zone, developed above the magma chambers after caldera collapse, is necessary to achieve the high gradients seen today. These models should help us understand recent bradyseismic events and future unrest.

Introduction

The Campi Flegrei caldera (CFc; Fig. 1), an active caldera that has shown signs of unrest in the last 30 years, hosts with its surroundings a population of more than one million people. Therefore, the volcanic risk of the area is very high. Any attempt to forecast the future activity of the volcano implies the knowledge of the present state of its magmatic system.

The CFc includes a continental and a submerged part and results from at least two large collapses related to the Campanian Ignimbrite (CI; 37 ka; Deino et al., 1992; 1994) and the Neapolitan Yellow Tuff (NYT; 12 ka) eruptions, respectively (Orsi et al., 1992, 1996). An ongoing resurgence has affected the NYT caldera since 10 ka and has generated the disjointing of the caldera floor in blocks, each with differential long-term vertical displacement. The unrest episodes that occurred in the last 30 years are short-term deformational events during the long-term resurgence process.

The magmatic system is still active as testified by the last eruption occurred at Monte Nuovo in 1538 (Di Vito et al., 1987), the widespread fumarolic and thermal springs activity

(Allard et al., 1991) and the recent unrest episodes (Casertano et al., 1976, Barberi et al., 1984, 1989; Orsi et al., 1999, this vol
ume). The existence of a magma chamber beneath the caldera has been postulated by Barberi et al. (1978), Armienti et al. (1983), Di Girolamo et al. (1984), Rosi and Sbrana (1987), Villemant (1988) and Civetta et al. (1991), and is likely located at shallow depth (4-5 km) (Ortiz et al.,1984; Ferrucci et al., 1992; De Natale and Pingue, 1993). Petrological and isotopic data (Pappalardo et al., 1999, this volume; D'Antonio et al., 1999, this volume) show that the magmatic system in the last 50 ka has behaved as an open system being refilled many times. Orsi et al. (1992, 1995) have shown that the reservoir was refilled by variable batches of magma before the NYT eruption.

The aim of this paper is to demonstrate numerical models of heat flow within the caldera and associated rocks that simulate the thermal regime measured in geothermal boreholes. These models, building on earlier works by Giberti et al. (1984), Bonafede et al. (1984), and Bonafede (1990) are constrained by known geological, geochemical, and geophysical properties and help to understand the magmatic history of the Phlegraean system and its present thermal state. While the results of these models are not unique, they certainly provide a basis by which one can evaluate the effects of various magma chamber geometries, sizes, ages, and intrusion histories. As a result of evaluating several models that best fit known constraints, we then can make interpretations about future behavior of the Campi Flegrei caldera system.

Further background covering geologic history, magma characteristics, and geophysical data for this study is given in Appendix A. The thermal modeling technique applied (HEAT) is summarized in Appendix B.

Model Constraints Based on Geology, Geochemistry, and Geophysics

From the preceding review and that included in Appendix A, we summarize the important boundary conditions that must be included in our thermal models.

(1)   The caldera results from two nested large collapses occurred at 37 and 12 ka, respectively.
(2)   The older caldera, related to the CI eruption, has a mean topographic diameter of about 16 km.
(3)   The younger caldera, related to the NYT eruption, is located in the central part of the older one and has a mean diameter of about 10 km.
(4)   Based upon the extensive studies by Smith and Shaw (1975; 1979) and Smith et al. (1978), the Phlegraean calderas are underlain by crustal magma bodies that have a diameter similar to that of the calderas.
(5)   The volume of these magma chambers is unknown, but Smith (1979) and other workers, such as Crisp (1984), have shown the magma chamber volumes can be constrained by the volume of caldera-eruption products. Typically for silicic eruptions, the chamber volume is larger than caldera-eruption products by a factor of 10 (Smith and Shaw, 1979).
(6)   The erupted volumes of magmas for the CI and NYT caldera-forming eruptions are estimated to be about 200 and 50 km^3, respectively. We assume a maximum volume of magma in the chamber before caldera eruptions of 2000 and 500 km^3, respectively; we also consider reasonable minimum chamber volumes of 1000 and ~160 km^3, based upon geometric assumptions, discussed below.

(7) CI varies in composition from alkali trachyte to trachyte, while NYT have composition variable from alkali trachyte to latite; in general these magmas have a density of about 2300 kg/m^3 (e.g. Wohletz et al., 1995) and thermal conductivities of about 2.8 W/m-K (Chelini and Sbrana, 1987; Wohletz and Heiken, 1992)

(8) Sr isotopic data (Fig. 2) gives evidence that the Phlegraean magmatic system was not a closed system, but it was periodically replenished by isotopically distinct trachytic and latitic magmatic batches. Accordingly, the magma chambers developed over a period of time and likely varied in volume and thermal structure.

(9) The depth of these magma chambers can only be constrained by one geophysical datum, PSv velocities indicating a chamber depth of 4 km; to be sure, the depth could be greater, but as we show later, the youth of magmatism and the high surface thermal gradients indicate very shallow magma chambers, even if hydrothermal convection has been important.

(10) The host rocks of these magma chambers is constrained by regional geology and gravimetric models (Fig.3; AGIP, 1987; Cassano and La Torre, 1987); accordingly we consider a general model of the deep stratigraphy (Chelini and Sbrana, 1987) consisting of carbonate rocks (density ~2650 Mg/m^3, conductivity ~1.0 W/m-K) to a depth of about 10 km; mafic igneous rocks (density ~2850 Mg/m^3, conductivity ~ 3.0 W/m-K) from 10 to 20 km, and crystalline metamorphic rocks (density ~3300 Mg/m^3, conductivity ~2.0 W/m-K) deeper than 20 km. Of these rocks, only the carbonate rocks may have porosity; however in the Phlegraean area, we have assumed negligible porosity.

(11) The near-surface stratigraphy consists of calc-alkaline and alkaline volcanic rock cover that now may have an accumulated thickness of several km, consisting of extruded rocks from magmatic systems developed in the Phlegraean area; however, as an initial condition, for our models, we assume no volcanic cover prior to development of large crustal magma chambers. New studies performed after completion of this study have shown that carbonate rocks may be missing in the Phlegraean area, but this information will have to be addressed in future modeling studies.

(12) The estimated amount of collapse for the CI and NYT calderas is 700 and 600 m (Fig. 3), respectively; collapses have been filled by pyroclastic and shallow marine deposits. In our modeling we have simplified each collapse to be 1 km and caldera fill to be generally trachytic in composition with an effective porous density of 2000 kg/m^3 and conductivity of 2.8 W/m-K, noting that near-surface tuffs may have greater porosity and lower conductivities (0.4 to 0.9 W/m-K; Corrado et al., 1998). The porosity of the caldera fill was periodically saturated (Chelini and Sbrana, 1987).

(13) The thermal gradient is an important part of the solution of the heat flow equation [Appendix B, Equation (B1)] and must be considered for initial conditions for numerical solutions, because it determines rates of heat diffusion by conduction during initial stages of magma chamber formation. The initial thermal gradient for the Phlegrean area can be extrapolated to 30°C/km from the regional gradient for this area of Italy given by Della Vedova et al. (1991).

(14) Surface geothermal manifestations (e.g., Solfatara) and evidence from deep drilling (Rosi and Sbrana, 1987) indicate that hydrothermal convection was likely pervasive within the caldera fills. The duration of hydrothermal convection is unknown but it has been largely arrested presumably by sealing of porosity by secondary minerals. Renewed faulting has caused hydrothermal convection to persist in some areas, most notably at Solfatara and Mofete. At Mofete, the geothermal gradient shows a strong convective signature. Recent studies now reveal hydrothermally altered lithic clasts from rocks older than the CI,

4

evidencing that a geothermal system existed before 37 ka; however, the location and extent of such a system cannot be constrained for our modeling.

Based on the above evidence, we develop our thermal models to include all of the above constraints and boundary conditions. In addition, we note the magmatic history dictates evolving boundary conditions that also must be included in thermal models. We summarize the general magmatic evolution here.

There is evidence of periodic magmatic activity prior to CI from both surface/subsurface geology and radiometric dates for several tens of thousands of years (Cassignol and Gillot, 1982), and recent age determinations have documented activity as early as 60 ka (Pappalardo et al., 1999, this volume). We assume that the magma chamber acquired its maximum volume just before CI eruption, based on isotopic data ka (Pappalardo et al., 1999, this volume), showing that by about 44 ka injection of new magma pulses had brought the isotopic composition of the magma chamber to those values characteristic of the CI, the most voluminous magmatic extrusion. The following list summarizes important extrusive events.

(1) At 37 ka the CI eruption produced caldera collapse over an area with an average diameter of 16 km. Estimated volume of erupted magma around 200 km^3 DRE. Composition of erupted magma is trachytic with constant $^{87}Sr/^{86}Sr$ ratios around 0.7073. Average diameter of the collapsed area about 16 km. Collapse depth about 700 m. Caldera fill composed of about 1000 m of trachytic subaerial and subaqueous tuffs and tuffites.

(2) Between 37 and 16 ka bp scattered eruptions extruded small (?) volumes of magma with constant trachytic composition and $^{87}Sr/^{86}Sr$ ratios similar to that of the CI. Around 16 ka bp, emplacement of the upper part of the Tufi Biancastri sequence through eruptions of trachytic magma with $^{87}Sr/^{86}Sr$ ratios similar to the NYT values. NYT shows three magma types consisting of two distinct isotopic compositions. Because the first extruded NYT magma appeared at 16 ka, we can assume the NYT chamber began to develop prior to that time. Without further constraints, the simplest model for evolution of the NYT chamber is that it involved two or three injections of magma spread out over a period of time from 12 ka back to a time as early as 28 ka, with early injections stimulating post-CI magmatic resurgence.

(3) Neapolitan Yellow Tuff eruption and caldera collapse occurred at 12 ka. Estimated volume of the erupted magma around 40-50 km^3 DRE. Orsi et al. (1991) proposed that three layers of magma existed in the chamber at the time of the eruption with the lowermost entering the chamber just before the eruption, but the NYT magma did not mix with the CI magma. The composition of the erupted magma is trachytic with the last erupted magma showing a composition varying from trachytic to latitic. The average diameter of the collapsed area about 10 km. Collapse depth around 900 m. The caldera fill composed mostly of trachytic subaqueous and subaerial tuffs and tuffites.

(4) D'Antonio et al. (1999, this volume) present geochemical and isotopic evidence that the most recent NYT magma system consists of a complex reservoir, filled by residual portions of the CI and NYT magmas, with the involvement of a third, deeper reservoir supplying less evolved magmas. This system generated many smaller and shallower pockets of evolved magma that fed most eruptions over the past 12 ka. These late stage eruptions, which are volumetrically minor, are associated with tectonic and hydrothermal events, summarized here:

- Around 10 ka bp eruption of trachybasaltic magma began at Minopoli. We have found that what was called Minopoli actually is the product of two eruptions, which we have called Minopoli 1 and Minopoli 2. The age of Minopoli 1 is bracketed between 10.7 and 10.3 ka, while that of Minopoli 2 must be between 10.3 and 9.5 ka (Di Vito et al., 1999, this volume).
- Around 10 ka bp resurgence began inside the NYT caldera, which has generated the uplift of the La Starza block of about 90 m.
- The last eruption occurred at Monte Nuovo in 1538 AD.
- Geothermal drilling at Mofete (at the intersection of faults related to resurgence) shows that an extensive hydrothermal convection system extended from depth to the surface for several ka, perhaps beginning at about 10 ka when resurgence began.
- 1970-72 and 1982-84 bradyseismic events occurred with a maximum net uplift of 3.5 m around the town of Pozzuoli.

Using the above initial conditions and time-dependent boundary conditions for our models, we have calculated over 50 different models, using HEAT, a 2-D finite difference, graphically interfaced code, described in Appendix B. The criteria for suitability of these models not only involves the geological similarity of our boundary conditions but also how well these models predict the measured, present-day, thermal gradients in the Phlegraean area, which extend to a maximum depth of ~3 km (AGIP, 1987). These thermal gradients have been measured in geothermal exploration boreholes at Licola (outside both calderas to the northwest), at San Vito (on the northeastern edge of the NYT caldera), and Mofete (on the inner side of the NYT western caldera rim). These thermal gradients are shown in Figure 4. Of these numerous models, we choose six types, summarized in Table 1, consisting of 12 individual models to demonstrate the primary controls of the thermal evolution (those being the magma chamber size, shape, and convective regimes). The primary magma chamber shapes we have studied are illustrated in Figure 5.

Model Results

For discussion of the thermal model results, we describe those models listed in Table 1 in order to illustrate the affects of magma chamber shape (Fig. 5), size, injection and cooling history, volcanic structure, and convective regimes upon the modeled thermal gradients. These gradients are shown in Figures 6-19, and Table 1 shows a comparison of temperatures at a depth of 2 km for the models and averaged measured data for each well.

An important step was definition of Model 0, which defines characteristic times for simple conductive cooling of a magma chamber system consisting of both the >37 ka Campanian Ignimbrite (CI) magma chamber and >12 ka Neapolitan Yellow Tuff (NYT) chamber. Modeled conservatively as 1000 km^3 in volume, cylindrical in shape, with a top near 4 km, this system produces maximum surface thermal gradients after 350 ka of cooling and requires ~600 ka to cool below 650° C. In summary, this model alone indicates in simplicity that the Campi Flegrei magmatic system still contains molten rock today and that hydrothermal convection must have played an important role in generating the high geothermal gradients monitored in boreholes.

Model 1: Simple Magma Bodies No Caldera Convection

Model 1 is a simple representation of the CI and NYT chambers with cylindrical shapes of 16 and 10 km diameter, respectively, each emplaced instantaneously at 37 and 12 ka, respectively. In addition, post-caldera activity at Minopoli is represented by injection of about 0.4 km^3 of trachytic basalt at the base of the NYT chamber. The volcanic structure modeled is represented by collapse of 1 km over the total diameter of the CIc at 37 ka and over the total diameter of the NYTc at 12 ka. This model was allowed to cool for a total of 37 ka, and no hydrothermal convection occurs within the caldera structures with the exception of that known to have happened along the Mofete fracture zone, for which the model has included a small area of 1 km wide extending from the surface to a depth of 0.5 km, active over the last 8 ka. This fracture zone likely represents movement caused by documented caldera resurgence (Orsi et al., 1996, 1999, this volume; Di Vito et al., 1999, this volume).

Figure 6 shows Model 1 thermal gradients to be much lower than those measured in geothermal boreholes at Licola, Mofete, and San Vito, which are quantified in Table 1. The modeled gradients are generally linear to a depth of 2.5 km with the exception of Mofete where convection has produced a vertical gradient from 0.5 to 1.0 km. These results while geologically viable (with the exception of magma injection history) demonstrate that more heat has to flow into surface rocks in order to match the data better.

This model was repeated using larger magma chambers by extending them to greater depths so that the CI chamber volume is 2000 km^3 and the NYT chamber is 470 km^3. As Table 1 shows, the results are the same as for smaller chambers, because the heat contained in the extra volumes at depth does not have time to diffuse and convect upward enough to significantly add heat to near surface rocks.

Model 2: Caldera Convection

It is clear from Model 1 that cooling times are much too short for conductive heat flow to raise the temperature of near surface rocks to measured values. In order to address this problem, we repeated Model 1 with the addition of caldera-collapse related hydrothermal convection in fractured rocks directly below the caldera fill material. Being a much larger caldera eruption, we modeled the CI caldera-related convection to extend 1 km below the CIc fill but only 0.5 km below the smaller NYTc fill. Model 2 was also repeated for larger magma chambers as was done for Model 1.

Figure 7 shows the pronounced affect of caldera-collapse related hydrothermal convection upon near-surface thermal gradients when compared to Model 1 (Fig. 6). Note that Licola gradients show very little affect of the caldera-related convection, because Licola is located outside of the CI caldera and hence has no convective regime beneath it. While the San Vito gradient nearly matches the measured gradient in the upper 1.5 km, it is too low at greater depth. The modeled Mofete gradient closely fits measured data. Again Model 2 using larger (deeper) magma chambers made little difference in the near surface gradients (Table 1).

Model 3: Incremental Intrusion

Because caldera-related hydrothermal convection included in Model 2 produce results tending toward better matches of thermal gradients, we include in Model 3 the more realistic approach to emplacement of magma in the CI and NYT chambers. This more realistic approach is based upon stratigraphic and radiometric age dates obtained thus far that show magmatism starting at by 50 ka (before the CI). For Model 3 we have emplace 1000 km^3 in 5 pulses starting at 57 ka, and thereafter every 5 ka with the CI chamber reaching its maximum volume just prior to the CI eruption at 37 ka. Furthermore, as discussed above, radiometric dates on magmas isotopically identical to the NYT show that the NYT magma existed before 16 ka. That fact along with the 3 distinct compositions of NYT magma erupted allows us to model the NYT magma chamber as beginning to form at 28 ka and reaching its full size just prior to 12 ka.

Figure 8 shows a graphical representation the calculational mesh boundary constraints for latest times of Model 3 and the thermal plot for present time. In Figure 8 thermal plot, a cross section of the magma chamber shows it to be dominantly above 800°C at present time with hotter magma of the NYT chamber centered at the top of the larger CI chamber. Note the upward bowed isotherms at Mofete. Figure 9 shows Model 3 thermal gradients with some improvement of modeled gradients at all locations, showing the affect of longer times for heat to flow from the chambers to the surface. Still it is apparent that caldera margin location (Licola and San Vito) are too cool at depth.

In order to demonstrate the temporal development of thermal gradients over the Phlegraean magma chamber system, Figure 10 depicts thermal gradients predicted at San Vito from initial conditions (30°C/km) through times at 37 ka (CI caldera eruption), 28 ka (first injection of magma into the NYT chamber), 20 ka, 12 ka (NYT caldera eruption), 8 ka (Minopoli intrusion), 4 ka (cessation of hydrothermal convection), and present time. Note the vertical gradients depicted for 28 ka until 4 ka, which are the product of hydrothermal convection. The thermal gradient increases through time until 4 ka after which the gradient relaxes to it present state because hydrothermal convection has stopped.

Model 4: Funnel Shaped Chamber with Domed Top

For Model 4 we attempt to remedy lack of heat at the caldera margins (e.g., Licola and San Vito) by concentrating more magma near the surface, using a funnel-shaped magma chamber. To accomplish this task we make the assumption that the CI magma chamber is like an inverted tear-drop shape such that most of the volume of the chamber is concentrated in the upper few kilometers of the chamber top. In addition for Model 4 we model this chamber to have a dome-like top, which might result from stoping near the top of the chamber. Other than this change in assumed chamber shape, all other parameters are the same as in Model 3, the most important being the hydrothermal convection below the caldera fill and the filling of the CI and NYT chambers over a prolonged period of time.

Two important variations of Model 4 (Models 4a and 4b) are described in Table 1. For Model 4a the filling of the CI chamber is lengthened to 50 ka, starting at 87 ka with magma added in pulses every 5 ka until maximum volume of 1000 km^3 is reached at 67 ka. Then a period of 20 ka occurs during which the chamber cools and leaks lava/tephra until 37 ka when

the chamber is replenished with fresh magma at its top, just prior to caldera eruption. For Model 4b, we explore the possibility that the CI chamber is emplaced with its top at 3 km starting at 56 ka, and at 37 ka its caldera eruptions produce collapse leaving the chamber top at a depth of 4 km.

Figures 11-13 show the resulting thermal gradients predicted by Model 4 variations. Model 4, while concentrating more heat near the center of the caldera and producing a very good match for the gradient at Mofete, does not produce high enough gradients at caldera margins shown by low predicted gradients for Licola and San Vito (Fig. 11, Table 1). This result is consistent with the domed-top of the CI magma chamber, which leaves the outer top margins of this chamber at a crustal depth of 5 km or more; hence, their is not enough cooling time for heat to diffuse towards the surface, even though the system has cooled for 57 ka. Prolonging this cooling time to 87 ka in Model 4a (Fig. 12) greatly helps this heat deficiency at San Vito where the predicted fit nearly exactly matches the measured data. Still predicted heat flow at Licola is too low and that at Mofete, which was nearly perfect in Model 4 is now too high in Model 4a. Applying another strategy of making the heat source closer to the surface, Model 4b (Fig. 13) produces yet a better fit of thermal gradients at Licola, but they are still on the low side. In addition, Model 4b demonstrates by much too high gradients at Mofete and San Vito at depths below 1 km, that making the CI chamber at a depth of 3 km until its caldera collapse is likely not geologically correct.

Model 5: Funnel-Shaped Chamber with Flat top

Since prolonging the cooling time of the CI chamber by increasing its age or making its roof closer to the surface do not produce results showing desired affects, Model 5 addresses the chamber shape by making it a funnel (inverted cone) with a flat top, which concentrates its heat nearer the surface along the margins of the chamber(Figure 14). The emplacement history of this model is the same as that in Model 4 as are other important factors such as the hydrothermal convection history. Model 5 includes one important variation, called Model 5a. This variation involves increasing the magma intruded during the Minopoli eruption to ~40 km^3 at the base of the NYT chamber with an associated dike protruding to the top of the chamber along its northeastern side below the vicinity of Minopoli.

Figure 14 also shows a thermal plot of present time predicted by HEAT for Model 5. Note the vestiges of increased hydrothermal convection at Mofete and the broad shoulders on isotherms above the magma chamber. A plot of thermal gradients predicted by Model 5 is shown in Figure 15, which displays very adequate fits to measured gradient data. Noting that the predicted gradient at San Vito falls below temperatures measured there, the model variation made for Model 5a (Table 1) provides extra heat flow in the area of San Vito by the intrusion associated with Minopoli (Fig. 16). This model produces gradients that are within 10 degrees of all measured data with exception of Licola at a depth of 2 km where the predicted temperature are ~27 degrees too low.

Figure 17 demonstrates the variation in thermal gradients at Mofete and San Vito during cooling of the Phlegraean magma system. In Figure 17a the effects of caldera-related hydrothermal convection are displayed by the vertical gradients at 28 and 12 ka, while the affect of convection at Mofete is show by the gradient at 4 ka. Since hydrothermal convection at

Mofete was stopped at 4 ka in Model 5a, the resulting present-day thermal gradient is relaxed back to much lower values that match measurements. Figure 17b demonstrates a gradual increase in thermal gradients with cooling time at San Vito, again dominated by the effects of hydrothermal convection beneath caldera fill.

Model 6: Spheroidally Shaped Chamber

Model 6 represents our attempt to model a more spherical magma chamber shape as another possible configuration. In this model, the chamber is an oblate spheroid, which represents the accumulation of magma in density stratified crustal host rocks. With the top of the spheroid at 4 km depth, this shape concentrates more magma at depth than in previous models. In order to match this chamber with the margins of the CI caldera, we have made its full diameter 20 km at a depth of 7.5-8 km, and its diameter 16 km at 5.5 km depth. This shape then has a total volume of magma at ~1750 km^3, but much of that is at considerable crustal depth. Hence in order to transport sufficient heat to the surface, a much longer cooling time is required. For this reason we begin to fill the chamber at 117 ka and add more magma every 20 ka until it reaches its maximum volume just prior to the CI caldera eruption at 37 ka. Other parameters for this model are the same with the NYT chamber filling the top of the CI chamber after it had erupted the CI magma.

Figure 18 shows the mesh design a present-day thermal plot for Model 6. Thermal gradient results shown in Figure 19 demonstrate a good match for the measured data at Mofete. At San Vito while the upper portion of the predicted gradient matches measured data, the gradient is too low at a depth greater than 1.7 km. The predicted gradient for Licola is much too low. This model demonstrates that the spheroidal shape does not put enough of the heat source near the surface below the caldera margins. If the cooling history were prolonged to get more heat to the surface below the caldera margins, then the center of the caldera would become to hot.

Discussion

Of the six model variations of over 50 completed, Model 5a, which involves cooling of an funnel-shape magma chamber with a flat top at a depth of 4 km below the Campi Flegrei predicts nearly identical thermal gradients to those measured in geothermal boreholes, showing an average difference in temperature at a depth of 2 km of only 19 degrees. The boundary conditions applied to this model conform to all geological, geochemical, and geophysical data that are presently. In applying this model to predicting future heat flow and resulting ground deformation in the Campi Flegrei, we acknowledge that there are still important boundary conditions that are only poorly constrained:

- Crustal stratigraphy
- The shape of the magma chambers
- The volume of the magma chambers
- The overall depth of the magma chambers
- The intrusion history of chamber filling
- The location and duration of hydrothermal convection

For our models, we assumed the crustal stratigraphy for the Phlegraean area to be similar to that of the region, which is dominated by near surface carbonate rocks and higher density crystalline rocks at depths below 10 km. Carbonate lithics have yet to be found in Phlegraean extrusive rocks. Indeed, studies in progress indicate that carbonates might be entirely lacking in the Phlegraean area. This possibility comes from the fact that the tectonic history of the area is likely quite different that than in the area of Vesuvius, which rests upon a completely different tectonic block. If carbonates are indeed missing from the crust in Campi Flegrei, the most likely near-surface rock type is calc-alkaline volcanic material. Carbonates generally have thermal conductivities much lower than those of calc-alkaline rocks and can be considered more as crustal "insulators." As such they tend to produce higher gradients in the near surface than would calc-alkaline rocks. For this reason, our models are conservative in the volume and depth of magma in the Phlegraean area needed to produce the measured geothermal gradients.

To our knowledge there is little or no information about the shape of alkaline, caldera-related magma chambers. Certainly the crustal stress distribution and density structure play a role in determining the actual shape of the Phlegraean magma system. The funnel shape that produced the best model results is perhaps the shape most readily defended by studies of calc-alkaline magma bodies, which show this characteristic shape often described as a inverted tear-drop shape. If magma rises like a diapir and flattens as it encounters a crustal density contrast near the level of its neutral buoyancy, the funnel shape might be expected [we note average calculated trachytic magma densities of ~2500 kg/m^3 (Wohletz et al., 1995) compared to those typical of carbonate rocks in the range of 2300 to 2700 kg/m^3 (Daly et al., 1966), which suggest neutral buoyancy within the hypothesized carbonate rock strata]. If one considers the extensional tectonic regime that likely dominated the Phlegraean area prior to CI magmatism, then one might be able to justify a more cylindrical chamber shape where magma rises below a regional horst. Even less credible is the spheroidal shape.

As discussed earlier, magma chambers volumes are best constrained by caldera-related extrusive volumes. It should be safe to assume that the magma chambers are of a larger volume than their caldera-related extrusions, but by how much remains unknown. Only the extensive studies by Smith and Shaw place some constraint on this issue—that being the magma chamber is about 10 times larger in volume that its caldera related eruptions [averaged for all the locations studied by Smith and Shaw (Smith and Shaw, 1975; 1979; Smith et al., 1978)]. Accordingly we have modeled the CI and NYT chambers at about this proportional size but have considered models for smaller and larger sizes (smaller sizes do not add enough heat to the crust to explain measured gradients satisfactorily). In looking at the thermal plots for these models, it is apparent that they are of enormous size compared to the familiar surface volcanic structures below which they remain. While researchers may disagree with these modeled chamber sizes, it is difficult to imagine other chamber configurations that satisfy the heat budget requirements, and thus the Smith and Shaw estimates appear to be justified, especially if convection above the magma chamber is minor.

The depth of the magma chambers modeled are only constrained by one datum, that is the PSv velocity transformation at 4 km below the Campi Flegrei (Ortiz et al., 1984; Ferrucci et al., 1992), which could correspond to the depth of still partially molten magma. Without further constraint at the time of writing, we note that if the magma chambers were deeper, then their age would have to be considerably older in order for sufficient heat to have been conducted or

convected to the surface. For our preferred funnel-shaped chamber model, the maximum depth is about 12 km, below which only the feeder dike system is present. For reference the regional background crustal thermal gradient of 30°C/km produces a 0.1 MPa wet-granite solidus temperature of 650°C at a depth near 22 km (shown as black on thermal plots referenced earlier), only several km above the Moho for this area of Italy (Crane et al., 1985).

For most models we have assumed the CI magma chamber began to grow about 57 ka bp. In support of this constraint are a few radiometric dates older than the CI rocks (*e.g*., 60 ka; Pappalardo et al., 1999, this volume), and rock chemistries indicating that the system was open, being replenished up to about 44 ka. To be sure, calc-alkaline volcanism likely existed in this area as far back as 1.5 Ma. We have demonstrated that prolonging the history of the magma chamber development provides additional time for heat to diffuse to the surface rocks, which is a needed parameter for relatively deep magma chambers to be viable sources for the heat flow in Campi Flegrei. If on the other hand, that Campi Flegrei has shallow magma chambers, then older systems would likely make the area much hotter than is presently known. The only way to address older shallow chambers by thermal modeling is to ignore evidence of hydrothermal convection.

For our models we settled upon configurations that required hydrothermal convection in the rocks directly beneath caldera fill materials. This constraint is based on knowledge of pervasive hydrothermal mineralization in well-bore samples from Campi Flegrei. In addition the geothermal gradients at Mofete display the characteristic slopes of those produced by a convective system. If hydrothermal convection were only a minor factor in the heat flow under Campi Flegrei, then to be sure, much larger chambers and/or longer cooling times have occurred. Modeling convective heat-flow in porous, saturated rocks is inexact, requiring assumptions regarding permeability effects of fracture fluid-flow. The important constraint on the maximum effect of fluid convection is that it cannot produce temperatures in excess of those driving the system at depth. In our models, the hydrothermal convection is driven by conductive gradients in rocks directly below the convective regime, rocks that overlie the magma chambers. The convective nature of the magma chambers we have modeled tends to make high magma temperatures persist at the tops of these chambers, which in turn drives heat flow in the roof rocks. It is possible that the variation in Sr isotopic compositions of CI samples reported Civetta et al. (1997) did result from interaction of the magma with hydrothermal fluids. Accordingly, we did investigate models where hydrothermal convection extended to the tops of the magma chambers, noting that if hydrothermal convection existed at these depths, it was likely to be present in near-surface rocks as well, because of the evidence that the calderas were periodically flooded by the sea and were filled with porous caldera-fill material. Results for these models show unrealistically high temperatures develop below the calderas where such convection was pervasive. If it were only confined to vent areas, then its effect on near surface gradients would be very limited.

Assuming the validity of these models (with exception of Model 0), we evaluated the state of magma remaining in the model chambers at present time. The average temperature of magma in these chambers (at depths less than or equal to 10 km) at present time ranges between ~820 to 870°C (Table 1). Furthermore, by assuming average liquidus and solidus temperatures for these magmas of 1000 and 700°C, respectively, and setting the liquid fraction as a function of magma temperature, we find that 74 to 84% of the remaining magma is in a liquid state (i.e., 15-

25% crystallized). Since for all models, at least 1000 km^3 of magma resides above 10 km depth, one can expect that over 700 km^3 remain in a liquid state below Campi Flegrei.

What are the volcanological implications for such predicted amounts of liquid magma? First, one might expect some kind of geophysical anomaly. At this point there is not seismic tomography for this area, but gravimetric and magnetic maps (AGIP, 1987) show localized anomalies. In review of the regional Bouguer anomaly map (e.g., Cassano and La Torre, 1987), only a small gravity minimum below Campi Flegrei, really no evidence of such a large body of molten rock. The total field magnetic map (reduced to the pole) shows only a small positive anomaly under Campi Flegrei, interpreted as part of the regional structural fabric, certainly not of any large consequence. These casual observations suggest that our estimations are incorrect, which is easily understood considering only the fact that we do not know the specific relationship between temperature and solid fraction for Phlegraean magmas. Secondly, if one accepts these estimations of liquid magma, then the chances for future large eruptions seems almost certain, perhaps only requiring a period of differentiation or additions of new magma to the existing chamber.

It is difficult to justify such volumes of liquid magma at depth with the lack of major geophysical anomalies, so we investigate models predicting the measured geothermal gradients but also resulting in a much lower volume of liquid magma remaining at present time. Such models require a much greater age for the magmatic system and/or smaller magma chambers, both of which cannot be constrained at this point. Our attempts at these kind of models involves developing the magma chamber of Model 5 and allowing it to cool ~470 ka before intrusion of new CI magma. We then modeled eruption of the CI and generally followed the scheme of Model 5 thereafter. While this model resulted in residual melts of about 470 km^3, it generated much too high geothermal gradients. Consequently, we developed another model, called Model 8, involving intrusion of 425 km^3 of pre-CI magma in a funnel shaped chamber with a cooling history of 300 ka. After this pre-CI magmatic event, Model 8 then involved intrusion of ~200 km^3 of CI magma just prior to the CI eruption. In Model 8 we also introduce the NYT magma in two pulses of 40 km^3 each at 20 and 12 ka, allowing the system then follow the same sequence of events as did Model 5. This model (Fig. 20) produced very satisfactory results as depicted in Figure 21. While predicting a residual liquid melt volume of ~200 km^3, Model 8 also generated thermal gradients nearly identical to the measured data, showing an average difference in temperature at a depth of 2 km of only 7 degrees.

While we cannot yet entirely justify our modeled pre-CI magmatic history with geological and geochronological data, we prefer Model 8 because it is more consistent with volcanic products older than the CI, which now are recognized but not analyzed. Model 8 also predicts much smaller amounts of residual crustal melt, which helps in reconciling the lack of major geophysical anomalies in the Campi Flegrei area.

Another volcanological implication for these thermal models concerns the issue of bradyseismic events. Orsi et al. (1999, this volume) has described a model for short-term deformations (bradyseismic) within the Campi Flegrei caldera. Their model involves rapid inflation events associated with intrusion of new magma pulses into the magma body. These events are rapid enough to produce some brittle failure of rock and seismic events. Such magma influxes certainly would produce finite but perhaps localized heat-flow perturbations and expansion of fluid volume.

Realizing that it is entirely possible that ~200 km^3 of liquid magma resides in the crust below Campi Flegrei and that the recent eruption history shows many small vents along the faults that border the resurgent block, one is faced with the likelihood that the future will show further eruptive activity.

In conclusion to our discussion of the thermal models, we emphasize the fact that these models are mathematically non-unique, that just because a model produces the correct results does not mean that it is the only possible model that might satisfy the present boundary conditions. It is for this reason, we investigated numerous models of varying boundary conditions, many of which produced adequate results. However, it was for only a fairly limited range of boundary conditions that results were clearly the closest fit to measured data. If more heat flow data were available, it is entirely possible that different models would be required to explain them. For example, it the measured gradients show high temperatures only because of very localized heat-flow highs, then smaller and/or deeper magma chambers might be viable.

Conclusions

Volcanologists are limited to understanding the present and past states of a volcanic field by evidences of surface morphology and eruptive processes. Only in old volcanic areas where erosion has exposed the plumbing system, and in some cases the underlying magma chambers, do researchers have a clue as to what subvolcanic systems look like. Where heat flow data exist in a volcanically active area, much can be learned by studying the heat flow processes to put constraints on what the heat source (magma chamber) is. Although 1-D analytical solutions to heat flow equations are useful as a first approximation, geologically viable solutions must include variable boundary conditions and non-linear terms of the heat flow equations. To this end we have produced many models of 2-D heat flow in attempt to understand possibilities for the state of magma chambers below the Phlegraean area. The petrographical, geochemical and isotopic data available on volcanic rocks representative of the CI and NYT eruptions have been integrated with geophysical and geological information in constraining our models.

Our main conclusions from this study, limited to our present knowledge of boundary conditions, are:

1. The measured geothermal gradients are predictable by the combined affects of conductive and convective (confined within the Campanian and NYT caldera margins) heat flow above the Phlegraean magma chamber system.
2. If magma chambers are not much older than their extrusive products, then maximum thermal pulse has not arrived at surface, and fluid convection in caldera rocks is required to explain the observed geothermal gradients.
3. Funnel-shaped chambers (Model 5 and Model 8) concentrate more of their heat near the surface and best explain geothermal data.
4. Increasing the magma chamber volume for relatively young chambers (i.e., < 60 ka) does not produce marked increases in surface gradients because there has not been enough time for heat transfer.

5. The Phlegraean area is presently underlain by large (at least 450 km^3) magma chamber system at an average temperature of about 740°C, which represents magma that is ~50% liquid.

These extensive efforts at modeling the heat flow for the Phlegraean magma system have helped us understand what information is critical in determining the nature of the Campi Flegrei volcanic field and its plumbing system. Based on these modeling studies, we are now much better prepared to critically evaluate what future geological, geochemical, and geophysical studies are necessary to help us refine thermal models necessary for hazard evaluation and risk mitigation.

Acknowledgements

Appendix A: Background

Geological History. The Campi Flegrei caldera (Fig. 1) has focused the interest of many scientists in the last two centuries (Breislack, 1798; Johnston Lavis, 1889; Dell'Erba, 1892; De Lorenzo, 1904). More recent papers have contributed to the definition of its evolution in the last 50 ka (Rittmann et al., 1950; Scherillo, 1953, 1955; Scherillo and Franco, 1960, 1967; Rosi et al., 1983; Di Girolamo et al., 1984; Lirer et al., 1987; Rosi and Sbrana, 1987; Barberi et al., 1991; Dvorak and Berrino, 1991; Dvorak and Gasparini, 1991; Scandone et al., 1991; Orsi et al., 1996).

The history prior to the CI eruption is poorly known. Rocks formed in this period are exposed only along the scarps bordering the Campi Flegrei and have been found in cores drilled north and east of the city of Napoli. The oldest dated among these deposits are from Torregaveta and Trefola quarry for which Pappalardo et al. (1999, this volume) obtained an age of about 60 ka; those authors also found evidence that pre-CI magmas were extruded episodically until 44 ka when they became chemically identical to that of the CI eruption.

The CI eruption (Di Girolamo, 1970; Barberi et al., 1978; Fisher et al., 1993; Rosi et al., 1995), the largest eruption of the Mediterranean area, extruded a volume of about 150 km^3 of magma ranging in composition from trachyte to phonolitic-trachyte (Civetta et al.,1996; 1997). Location of the eruptive vent has been debated in literature. A NW-SE trending fracture north-west of Napoli (Di Girolamo, 1970; Barberi et al., 1978; Di Girolamo et al., 1984) and the Acerra depression north-east of Napoli (Scandone et al., 1991) were suggested as source for the CI. Rosi et al. (1983, 1995), Rosi and Sbrana (1987) and Barberi et al. (1991) located the vent area in the Campi Flegrei. AMS flow direction data (Fisher et al., 1993) and evidence from surface and subsurface geology (Orsi et al., 1996) corroborate this hypothesis. The eruption was accompanied by a caldera collapse. (Rosi et al., 1983, 1995; Rosi and Sbrana, 1987; Barberi et al., 1991) which included the Campi Flegrei, the city of Napoli, the Pozzuoli bay and the northwestern part of the bay of Napoli (Orsi et al., 1996).

The volcanism between the CI and the NYT eruptions have generated mostly pyroclastic deposits and subordinately lava domes, either exposed or found in the subsurface (Di Girolamo et al., 1984; Rosi and Sbrana, 1987; Orsi et al., 1996), in the peripheral sector of the continental part of the caldera, and the volcanic edifices of the Pentapalummo and Miseno banks (Pescatore et al., 1984; Fusi et al., 1991) at the southern and southwestern margin of the caldera, in its submerged part.

The NYT eruption, the second largest of the Mediterranean area, emitted about 40 km^3 of magma with a composition variable from alkali-trachyte to latite (Orsi et al., 1992, 1995; Scarpati et al., 1993; Wohletz et al., 1995). It was accompanied by a caldera whose collapse began during the coarse of the eruption (Orsi et al., 1992). The caldera margin, not exposed, has been inferred by Orsi et al. (1996) from the distribution of gravimetric and magnetic anomalies (Barberi et al, 1991), vents younger than the NYT, dated level surfaces in its submerged part (Pescatore et al., 1984; Fusi et al., 1991), and from interpretation of deep drillings data (AGIP, 1987).

The volcanism younger than the NYT can be subdivided in three epochs of activity dated at 12-9.5, 8.6-8.2, 4.8-3.8 ka respectively (Di Vito et al., 1999, this volume). After a quiescence of about 3,000 years, in September 1538, the last eruption took place and formed Monte Nuovo. During the three epochs all the vents were located inside the NYT caldera and erupted magmas ranging in composition from trachybasalt, to latite, to trachyte to alkali trachyte. The eruptions occurred along regional faults, partially reactivated during the NYT caldera collapse and fed by trachybasaltic and latitic magmas (D'Antonio et al., 1999, this volume). The vents of the first epoch were located along the marginal faults of the NYT caldera. During the second epoch the vents were mostly located in the northern and eastern part of the NYT caldera. During the third epoch the vents were located in the northeastern sector of the

16

NYT caldera floor. Eruptions have never occurred inside the Pozzuoli bay that is in the central and southern parts of the NYT caldera.

Magma Characteristics . The CF rocks, classified according to the normative nepheline versus DI grid range in composition from trachybasalt, to latite, trachyte, alkali-trachyte and phonolitic trachyte with trachyte and alkali-trachyte being the most abundant. They form an almost continuous evolution series, with, however, a significant compositional gap between trachybasalt and latite. Figure 2 summarizes the compositional variation of the Campi Flegrei volcanic products through time.

Rocks older than CI are highly evolved, mostly alkali-trachyte and phonolitic trachyte, trachytic rocks have only been found in a core drilled at Ponti Rossi (Fig. 1). Estimates of the volume of erupted magma are difficult to be made, because the rocks constitute small and isolated exposures at the periphery of the CI caldera and occur in drilling cores. Both proximal (Breccia Museo and Piperno) and distal products erupted during the huge CI eruption are compositionally zoned. Three different magmas were emitted during this eruption: the earliest was alkali-trachytic (25 km^3 DRE), the second was a mingled alkali-trachytic to trachytic magma (100 km^3 DRE) and the latest was the least-evolved, trachytic magma (20 km^3 DRE).

Most of the volcanic products erupted between the CI and the NYT eruptions are buried inside the CI caldera. The composition of the analyzed rocks erupted during this period is dominantly alkali-trachytic, with the exception of the latitic Torre Gaveta deposit erupted at about 14 ka.

During the NYT eruption, three magmas with distinct composition were tapped: the first was alkali-trachytic, the second was trachytic and the third was compositionally zoned from alkali-trachytic to latitic. The total volume of erupted magma was estimated at about 50 km^3 DRE.

Volcanism younger than the NYT eruption, was mostly concentrated in three epochs of activity separated by periods of quiescence, as testified by the occurrence of two widespread paleosols. The three periods lasted between 12 and 9.5 ka, 8.6 and 8.2, and 4.8 and 3.8 ka, respectively. During the first epoch of activity mostly trachytic and alkali-trachytic magmas were erupted. The vents for these eruptions were located on the Averno-Capo Miseno alignment, the western rim of the NYT caldera, and along the eastern margin of the NYT caldera. Trachybasaltic and latitic magmas were erupted along the rim and outside the caldera depression, testifying the occurrence of a less differentiated magma body underlying the caldera. The products erupted during the second epoch are mostly trachytic and alkali-trachytic in composition, with subordinate trachybasaltic products .The vents for these eruptions occur in the western, northern and eastern sectors of the NYT caldera. During the third epoch, trachytic to phonotrachytic magmas were erupted from vents located inside the NYT caldera, along faults bordering the resurgent block, and the Averno-Capo Miseno alignment. The last eruption of the caldera occurred in September 1538, after a quiescence of 3 ka with the emission of phonolite-trachytic magma. ^{87}Sr/^{86}Sr ratios of the CF rocks range from 0.70679 to 0.7085. D'Antonio et al. (1999, this volume) characterize the present magma system as a complex reservoir filled by residual portions of the CI and NYT magmas, with the involvement of a third, deeper reservoir supplying less evolved magmas. This system has generated many smaller and shallower pockets of evolved magma that have fed most eruptions over the past 12 ka.

Geophysical Data. AGIP (1987) reported early geophysical data concerning the Phlegraean geothermal system, much of which has been related by Cassano and La Torre (1987). This early work showed a Bouguer anomaly and a velocity structure that well defined the Phlegraean caldera structure. A W-NE gravimetric profile (AGIP, 1987), shown in Figure 3, displays a 2-D density model for the gravimetric profile, which can be interpreted based on the existence of relatively less dense caldera-fill rocks in the upper 1 km of the caldera, underlain by progressively denser strata of earlier lavas and thermal metamorphic rocks at a depth below 3 km, just above the presumed magma chamber. Cassano and La Torre (1987) combine the gravimetric data with those of magnetic, magnetotelluric, and geoelectric surveys (Carrara et al., 1973; 1974) to provide a detailed schematic cross section of the caldera structure. Our working model of the caldera structure is based on these early studies and their interpretations provided by Rosi and Sbrana (1987) and Barberi et al. (1991).

Geothermal gradient drilling performed by AGIP (1987) and reported by Rosi and Sbrana (1987) as well as Chelini and Sbrana (1987) give perhaps the most important data for our study. These data shown in Figure 4, refer to three distinct areas explored by AGIP: Mofete, Licola, and San Vito. Chelini and Sbrana (1987) show that the highest gradients are found at Mofete where there is strong mineralogical indications of hydrothermal convection. While the

17

gradients measured at Mofete show a strong signature of convective heat flow, this affect is less apparent at San Vito and absent at Licola, drilled outside the caldera margin.

Based upon these geophysical evidences with conservative projections of geothermal gradients (which is certainly not appropriate for the Mofete area because of convective effects), a depth to the magma chamber top of 4 km or more is reasonable. More recently, Ortiz et al. (1984) and Ferrucci et al., (1992) have analyzed PSv seismicity to conclude that magma resides at a depth of 4 km below the Phlegraean caldera.

Appendix B: Thermal Modeling Technique

Quantitative study of heat transfer in geologic materials has evolved from those early considerations of Lovering (1935) through the elegant mathematical analyses provided by Carslaw and Jaeger (1947), the latter of which have become benchmark treatments most cited in geological literature. Numerical computational techniques now make solution possible for heat transfer equations that express multiple dimensions with nonlinear elements of rock heterogeneity, changing source character, and spatially and temporally varying convection. Examples of such applications are those by Kolstadt and McGetchin (1978) and Zyvoloski (1987), the latter of which introduces the detailed account for heat transfer in porous media. Review of such concepts are given in Furlong et al. (1991) and Turcotte and Schubert (1982).

While conduction dominates heat transfer in solid phases, convection is of great importance for fluid phases in porous media that are relatively permeable. A general mathematical expression for such heat transfer is given by the conservation of energy:

$$\rho_b C_b \frac{\partial T}{\partial t} = \nabla(K_b \nabla T) - \nabla \cdot (\rho_f C_f \cdot \mathbf{u}) + A \tag{B1}$$

where ρ and C are density and specific heat, respectively, T is temperature, K is rock conductivity, $\mathbf{u}$ is the convective velocity, and A represents heat loss/gain through radioactive decay, chemical reactions, and latent heat of crystallization and fusion. Subscripts b and f refer to properties in bulk (rock + fluid) and the fluid, respectively. Equation (B1) shows the temporal heat storage (left-hand side) equal to the conductive ands the convective fluxes, respectively taken together with a term for heat source/sinks. Ignoring the convective flux and heat source/sink terms in Equation (B1), we expand the conductive flux term in cartesian coordinates for two-dimensions:

$$\frac{\partial T}{\partial t} = \frac{\partial \kappa_x}{\partial x}\frac{\partial T}{\partial x} + \frac{\partial \kappa_z}{\partial z}\frac{\partial T}{\partial z} + \kappa_x \frac{\partial^2 T}{\partial x} + \kappa_z \frac{\partial^2 T}{\partial z} \tag{B2}$$

where κ is the thermal diffusivity. Nonlinearity results from heat diffusion not only reflecting local thermal gradients but also spatial variation of diffusivity with rock heterogeneity, temperature, and magma emplacement history.

Thermal conductivity varies with temperature and has been modeled by Chapman and Furlong (1991) as

$$K(T,z) = K_0 \left(\frac{1+cz}{1+bT} \right) \tag{B3}$$

For this equation thermal conductivity [$K(T, z)$] is a function of crustal depth (z) and temperature (T) where K_0 is conductivity at 0°C, c is the crustal depth constant equal to 1.5×10^{-3}/km, and b is the thermal constant equal to 1.5×10^{-3}/°C for the upper crust and 1.0×10^{-4}/°C for the lower crust. This function adequately describes variations in most common rock thermal conductivities with temperature and fits those data for most magmas (with exception of rhyolite) measured by McBirnery and Murase (1984).

In derivation of the convective flux term of Equation (B1) one must consider conservation of mass expressed by Parmentier (1979) for a steady state as

$$\nabla \cdot \left(\rho_f \mathbf{u}\right) = 0 \quad , \tag{B4}$$

where ρ_f is convecting fluid density, and conservation of momentum, commonly expressed by Darcy's law (e.g., Norton and Cathles, 1979; Cathles, 1983) expressed as

$$\mathbf{u} = -\frac{k\rho}{\mu}\left(\nabla p - \rho_f g\right) \quad , \tag{B5}$$

where $\mathbf{u}$ is the convective velocity, k is permeability, μ is the dynamic viscosity, p is pressure, and g is gravitational acceleration. The term in parentheses in Equation (B5) is the net fluid pressure gradient, and because the lithostatic pressure gradient is greater than the hydrostatic gradient by a factor of about 3, fluids at lithostatic pressure will tend to ascend and transport heat upwards. Pressure is given by and integrated form of Darcy's law:

$$p = \int_0^z \left(\rho g - \frac{\mu}{\kappa\rho}u_z\right)dz \quad , \tag{B6}$$

which shows that fluid pressure depends on fluid density and vertical flux. Finally the fluid equation of state is primarily a function of its coefficient of isobaric thermal expansion (α)

$$\rho = \rho_0\left(1 - \alpha\Delta T\right) \quad , \tag{B7}$$

where ρ_0 is the reference density of the fluid and ΔT is the temperature difference driving the flow. Because the vertical pressure gradient in a convecting fluid system is nearly hydrostatic ($\nabla p = \rho_0 g$) and convection is driven by the difference between the hydrostatic pressure gradient and that due to decrease fluid density at higher temperatures, the net pressure gradient is $\rho_0\alpha\Delta Tg$ and the vertical convective flux (Cathles, 1983) is then

$$u_z = \frac{k\rho}{\mu}\rho_0\alpha\Delta Tg \quad . \tag{B8}$$

Convection also plays a role in cooling of magma chambers, and as shown by many workers (e.g., Valentine, 1992) can be evaluated by the thermal Rayleigh number (Ra). Where Ra is between 10^3 and 10^5, magma chamber convection is likely and its overall influence on heat flow can be quantified by Nusselt number (Nu).

The major elements of heat sources for Equation (B1) are addition of new magma to the system and the latent heat of crystallization while heat sinks are magma chamber volume decreases by eruption and latent heat of fusion of host rocks around magma chambers and fusion of cooled old magma by injection of new magma. To calculate this effect, we consider crystallization and melting to occur over a range of temperatures between 650°C and 1000°C, which is appropriate for a wide range of magma compositions. For simplicity, we apply the assumption that melt fraction varies linearly with temperature over the above crystallization range and that an average latent heat for all phases is ~350 kJ/kg.

The most important aspect of numerical solution of Equation (B1) is determination of appropriate boundary conditions that represent geologic structure and locations of various host rock bodies, magma chambers, and zones of fluid convection. Since we know that these boundary conditions have changed over time for the Campi Flegrei, we developed a user-interactive graphical interface for a two-dimension numerical code, HEAT. Because numerical solutions of this kind are non-unique and because of inherent uncertainty in appropriate boundary conditions, such as magma chamber size, shape, and depth, a large number of model calculations have to be made in order to fully study the range of possible solutions. Such a task requires a tremendous amount of computational time, so we chose to study the problem in two-dimensions, such that full simulation for model times of over 100 ka could be reasonably achieved in less than an hour of computer time. As such, our solutions represent an assumed axisymmetrical system. The graphical interface of our code continuously updates thermal plots and allows replay of animations, showing

graphical representation of evolving thermal regime. To address temporally varying boundary conditions, the interface allows rezonation of the computational mesh at any time during the calculation.

Based on an earlier VMS version documented by Wohletz and Heiken (1992), the present version of HEAT has been considerably improved and tested on a wide variety of geologic structures and rock properties with both conductive and convective heat flow. In application of HEAT to the Campi Flegrei system we follow the method described by Stimac et al. (1997), who modeled the Clear Lake volcanic field in California. A version of HEAT has been adapted for laboratory rock melting experiments involving rocks melted by a moving hot molybdenum probe. Results thus far have shown that HEAT predicts temperatures within one percent of those measured by thermocouples, thus allowing detailed engineering designs to be made from the results of HEAT.

HEAT is a 32-bit application suitable for workstations operating Windows™ 95/98/NT. The graphical interface is readily used by the novice to develop and tailor the simulation to represent most geological conditions of magma intrusion and geological structure. HEAT employs an explicit finite differencing scheme. The time step used in calculations is dependent upon size of spatial discretization and is set to conservatively achieve the necessary Courant condition for stability. Truncation errors that might evolve when using very short time steps are minimized by utilizing double precision. Continuous thermal gradients are assigned along the boundaries and initial conditions use a designated regional thermal gradient. All rock/magma properties are assigned by the user and they include: density, porosity (fluid saturation), heat capacity, initial temperature, spatially and thermally varying thermal conductivities, and location. Latent heats of fusion/crystallization are solved for all rocks including magma where temperatures are in that range. Convective heat transfer in the magma bodies is determined by analysis of Ra for each body. Where the calculated Ra is sufficient for convection, convection heat flow is calculated as a function of temperature and composition reaching a maximum Nu values of 3 for silicic magmas and 10 for mafic magmas. Where fluid convection is modeled, it is assumed to occur in fractured rock. Because effective permeabilities of fractured rocks are not known for this area, high permeabilities are assumed such that convective heat flow is limited to an effective Nu of 100. As mentioned earlier, the code has been applied to several geologic areas to test its suitability.

The general method for application of HEAT involves initial sensitivity studies for variation in assumed host and magma rock properties, the most important being vertical and lateral conductivities, temperature, and density, magma chamber volume and depth, and the effect of spatial discretization. For this study over 50 models were calculated to cover a wide range of possible geologic boundary conditions and initial conditions. As described in earlier text, each of these models applied constraints derived from geological, geophysical, and geochemical studies (Orsi et al., 1996). So all the models had some geological validity, but only a fraction of the models are considered to be useful. The criteria for deciding the utility of model results is how well the models predict the present geothermal gradients documented in studies described.

References

AGIP, 1987. Modello geotermico del sistema flegreo (Sintesi). Servizi Centrali per l'Esplorazione, SERG-MESG, San Donato, 23 pp.

Allard, P., Maiorani, A., Tedesco, D., Cortecci, G. and Turi, B., 1991. Isotopic study of the origin of sulfur and carbon in Solfatara fumaroles, Campi Flegrei caldera. J. Volcanol. Geotherm. Res., 48 (1/2): 139-159.

Armienti, P., Barberi, F., Bizouard, H., Clocchiatti, R., Innocenti, F., Metrich, N., Rosi, M. and Sbrana, A., 1983. The Phlegraean Fields: Magma evolution within a shallow chamber. J. Volcanol. Geotherm. Res., 17: 289-311.

Barberi, F., Innocenti, F., Lirer, L., Munno, R., Pescatore, T. and Santacroce, R. 1978. The Campanian Ignimbrite: a major prehistoric eruption in the Neapolitan area (Italy). Bull. Volcanol., 41 (1): 1-22.

Barberi, F., Corrado, G., Innocenti, F. and Luongo, G., 1984. Phlegrean Fields 1982-1984: brief chronicle of a volcano emergency in a densely populated area. Bull. Volcanol., 47 (2): 175-185.

Barberi, F., Carapezza, M., Innocenti, F., Luongo, G. and Santacroce, R., 1989. The problem of volcanic unrest: the Phlegraean Fields case history. Atti Conv. Lincei, 80: 387-405.

Barberi, F., Cassano, E., La Torre, P. and Sbrana, A., 1991. Structural evolution of Campi Flegrei Caldera in light of volcanological and geophysical data. J. Volcanol. Geotherm. Res., 48 (1/2): 33-49.

Bonafede, M., Dragoni, M. and Boschi, E., 1984. Heat diffusion and size reduction of a spherical magma chamber. Bull. Volcanol., 47 (2): 343-347.

Bonafede, M., 1990. Axi-symmetric deformation of a thermo-poro-elastic half-space: inflation of a magma chamber. Gephys. J. Int., 103: 289-299.

Breislack, S., 1798. Topografia Fisica della Campania. Brazzini, Firenze, 368 pp.

Carrara, E., Iacobucci, F., Pinna, E. and Rapolla, A., 1973. Gravity and magnetic survey of the Campanian volcanic area, S. Italy. Boll. Geof. Teor. Appl., 15 (57): 39-51.

Carrara, E., Iacobucci, F., Pinna, E. and Rapolla, A., 1974. Interpretation of gravity and magnetic anomalies near Naples, Italy, using computer techniques. Bull. Volc., 38 (2): 458-467.

Carslaw, H.S. and Jaeger, J.C., 1947. Conduction of heat in solids. Oxford Univ. Press, Oxford, 386 pp.

Cassano E. and La Torre, P., 1987, Geophysics. In: M. Rosi and A. Sbrana (Editors), Phlegrean Fields. CNR Quaderni de "La Ricerca Scientifica", 114: 94-103.

Casertano, L., Oliveri, A. and Quagliariello, M.T., 1976. Hydrodynamics and Geodynamics in the Phlaegraean Fields area of Italy. Nature, 264:161-164.

Cassignol, C. and Gillot, P.Y., 1982. Range and effectiveness of unspiked potassium-argon dating: experimental ground work and application. In: G.S. Odin (Editor), Numerical Dating in Stratigraphy. Wiley, New York, NY. 160 pp.

Cathles, L.M., 1983. An analysis of the hydrothermal system responsible for massive sulfide deposition in the Hokuroku Basin of Japan. Econ. Geol. Monograph, 5: 429-487.

Chapman, D.S. and Furlong, K.P., 1991. Thermal state of the continental crust. In: Continental Lower Crust, Elsevier, Amsterdam.

Chelini, W. and Sbrana, A., 1987, Subsurface geology. In: M. Rosi and A. Sbrana (Editors), Phlegrean Fields. CNR Quaderni de "La Ricerca Scientifica", 114: 94-103.

Civetta, L., Carluccio, E., Innocenti, F., Sbrana, A. and Taddeucci, G., 1991. Magma chamber evolution under the Phlegraean Field during the last 10 ka; Trace element and isotopic data. Eur. J. Mineral., 3: 415-428.

Civetta, L., de Vita, S., Di Vito, M., Orsi, G. and Pappalardo, L., 1996. Geochemical and isotopic data of Campi Flegrei products older than 35 ka from a bore-hole drilling located in Campanian Plain. In prep.

Civetta, L., Orsi, G., Pappalardo, L., Fisher, R.V., Heiken, G.H. and Ort, M., 1997. Geochemical zoning, mixing, eruptive dynamics and depositional processes—the Campanian Ignimbrite, Campi Flegrei, Italy. J. Volcanol. Geotherm. Res., 75: 183-219.

Corrado, G., De Lorenzo, S., Mongelli, F., Tramacere, A. and Zito, G., 1998. Surface heat flow density at the Phlegrean Field Caldera (southern Italy). Geothermics, 27: 469-484.

Crane, W., Bonatti, E., Labrecque, J. and Bell, R., 1985. Bay of Naples Geophysical profiles. R/V Conrad C 2508, L-DG0, Tech. Rep.

Crisp, J.A., 1984. Rates of magma emplacement and volcanic output. Jour. Volc. Geotherm. Res., 20: 177-211.

Daly, R.A., Manger, G.E. and Clark Jr., S.P., 1966. Density of rocks. In: S.P. Clark, Jr. (Editor), Handbook of Physical Constants. Geol. Soc. Amer., Mem. 97, 19-26.

D'Antonio, M., Civetta, L., Orsi, G., Pappalardo, L., Piochi, M., Carandente, A., de Vita, S., Di Vito, M. A. and Isaia, R., 1999. The present state of the magmatic system of the Campi Flegrei caldera based on a reconstruction of it behavior in the past 12 ka. J. Volcanol. Geotherm. Res., this volume.

De Lorenzo, 1904. The history of volcanic action in the Phlegraean Fields. Q. J. Geol. Soc., 9.

Della Vedova B., Mongelli F., Pellis G., Squarci P., Taffi L. and Zito G., 1991. Heat-flow map of Italy. L. Gori (Editor), CNR - International Institute of Geothermal Research, Pisa, Italy.

Dell'Erba, L., 1892. Considerazioni sulla genesi del Piperno. Atti Acc. Sc. Fis. Mat., Napoli, 5, 22 pp.

Deino, A.L., Curtis, G. and Rosi, M.,1992. ^{40}Ar/^{39}Ar dating of Campanian Ignimbrite, Campanian Region, Italy. Int. Geol. Congress, Kyoto, Japan, 24 Aug.-3 Sept., Abstr., 3: 633.

Deino, A.L., Southon, J., Terrasi, F., Campajola, L. and Orsi, G., 1994. ^{14}C and ^{40}Ar/^{39}Ar dating of the Campanian Ignimbrite, Phlegrean Fields, Italy. Abstract ICOG, Berkley California USA.

De Natale, G. and Pingue, F.,1993. Ground deformations in collapsed caldera structures. J. Volcanol. Geotherm. Res., 57: 19-38.

Di Girolamo, P., 1970. Differenziazione gravitativa e curve ischimiche nella "Ignimbrite Campana" (Tuffo Grigio Campano auct.). Rend. Soc. Ital. Mineral. Petrol. 26: 1-45.

Di Girolamo, P., Ghiara, M.R., Lirer, L., Munno, R., Rolandi, G. and Stanzione, 1984. Vulcanologia e petrologia dei Campi Flegrei. Boll. Soc. Geol. It., 103: 349-413.

Di Vito, M.A., Lirer, L., Mastrolorenzo, G. and Rolandi, G., 1987. The Monte Nuovo eruption (Campi Flegrei, Italy). Bull. Volcanol., 49:608-615.

Di Vito, M.A., Isaia, R., Orsi, G., Southon, J., D'Antonio, M., de Vita, S., Pappalardo, L. and Piochi, M., 1998. Volcanic and deformation history of the Campi Flegrei caldera in the past 12 ka. J. Volcanol. Geotherm. Res., this issue.

Dvorak, J.J. and Berrino, G., 1991. Recent ground movement and seismic activity in Campi Flegrei, Southern Italy: episodic growth of a resurgent dome. J. Geophys. Res., 96: 2309-2323.

Dvorak, J.J. and Gasparini, P., 1991. History of earthquakes and vertical movement in Campi Flegrei caldera, Southern Italy: comparison of precursory events to the A.D. 1538 eruption of Monte Nuovo and activity since 1968. J. Volcanol. Geotherm. Res., 48: 77-92.

Ferrucci, F., Hirn, A., De Natale, G., Virieux, J. and Mirabile, L., 1992. P-SV conversions at a shallow boundary beneath Campi Flegrei caldera (Italy): evidence for the magma chamber. J. Geophys. Res., 97-B11: 15,351-15,359.

Fisher, R. V., Orsi, G., Ort, M. and Heiken, G. 1993. Mobility of a large-volume pyroclastic flow - emplacement of the Campanian ignimbrite, Italy. J. Volcanol. Geotherm. Res., 56: 205-220.

Furlong, K.P., Hanson, R.B. and Bowers, J.R., 1991. Modelling thermal regimes. In: D. Kerrick (Editor),Contact Metamorphism. Rev. Mineral., 26: 437-506.

Fusi, N., Mirabile, L., Camerlenghi, A. and Ranieri, G., 1991. Marine geophysical survey of the Gulf of Napoli (Italy): relationships between submarine volcanic activity and sedimentation. Mem. Soc. Geol. It., Spec. Paper.

Giberti, G., Moreno, S. and Sartoris, G., 1984. Thermal history of Phlegraean Fields (Italy) in the last 50,000 years: A schematic numerical model. Bull. Volcanol., 47 (2): 331-341.

Johnston Lavis, H.F., 1889. Report of Committee appointed for the investigation of the volcanic phenomena of Vesuvius and its neighbourhood (London).

Kolstad, C.D. and McGetchin, T.R., 1978. Thermal evolution models for the Valles caldera with reference to a hot-dry-rock geothermal experiment. Jour. Volcanol. Geotherm. Res., 3: 197-218.

Lirer, L., Luongo, G. and Scandone, R., 1987. On the volcanological evolution of Campi Flegrei. EOS, Trans. Am. Geophys. Union, 68: 226-234.

Lovering, T.S., 1935. Theory of heat conduction applied to geological problems. Geol. Soc. Amer. Bull., 46: 69-84.

McBirney, A.R. and Murase, T., 1984. Rheological properties of magmas. Ann. Rev. Earth Planet. Sci., 12: 337-357.

Norton, D. and Cathles, L.M., 1979. Thermal aspects of ore deposition. In: H.L. Barnes (Editor), Geochemistry of Hydrothermal Ore Deposits. Wiley, New York, 798 pp.

Orsi, G., D'Antonio, M., de Vita, S. and Gallo, G., 1992. The Neapolitan Yellow Tuff, a large-magnitude trachytic phreatoplinian eruption: eruptive dynamics, magma withdrawal and caldera collapse. J. Volcanol. Geotherm. Res., 53: 275-287.

Orsi, G., Civetta, L., D'Antonio, M., Di Girolamo, P. and Piochi, M., 1995. Step-filling and development of a three-layers magma chamber: the Neapolitan Yellow Tuff case history. J. Volcanol. Geotherm. Res., 67: 291-312.

Orsi, G., Del Gaudio, C., de Vita, S., Di Vito, M.A., Petrazzuoli, S.M., Ricciardi, G. and Ricco, C., 1999. Short-term ground deformations and seismicity in the nested Campi Flegrei caldera (Italy): an example of active block-resurgence in a densely populated area. J. Volcanol. Geotherm. Res., this volume.

Orsi, G., De Vita, S. and Di Vito, M., 1996. The restless, resurgent Campi Flegrei nested caldera (Italy): constraints on its evolution and configuration. J. Volcanol. Geotherm. Res., 74: 179-214.

Ortiz, R., Arana, V., Astiz, M. and Valentin, A., 1984. Magnetotelluric survey in the bradyseismic area of Campi Flegrei. Bull. Volcanol., 47: 239-246.

Pappalardo, L., Civetta, L., D'Antonio, M., Deino, A., Di Vito, M., Orsi, G., Carandente, A., de Vita, S., Isaia, R. and Piochi, M., 1999. Chemical and Sr-isotopical evolution of the

Phlegraean magmatic system before the Campanian Ignimbrite and the Neapolitan Yellow Tuff eruptions. J. Volcanol. Geotherm. Res., this volume.

Parmentier, E. M., 1979. Two phase natural convection adjacent to a vertical heated surface in a permeable medium. Int. J. Heat Mass Trans., 22: 849-855.

Pescatore, T., Diplomatico, G., Senatore, M.R., Tramutoli, M. and Mirabile, L., 1984. Contributi allo studio del Golfo di Pozzuoli: aspetti stratigrafici e strutturali. Mem. Soc. Geol. It., 27: 133-149.

Rittmann, A., Vighi, L., Falini, F., Ventriglia, V. and Nicotera, P., 1950. Rilievo geologico dei Campi Flegrei. Boll. Soc. Geol. It., 69:117-362.

Rosi, M. and Santacroce, R., 1984. Volcanic hazard Assesment in the Phlegraean Fields: a contribution based on stratigraphic and historical data. Bull. Volcanol. 47 (2): 359-370.

Rosi, M. and Sbrana, A., 1987. Phlegrean Fields. CNR, Quaderni de "La Ricerca Scientifica", 114: 1-175.

Rosi, M., Sbrana, A. and Principe, C., 1983. The Phlegrean Fields: structural evolution, volcanic history and eruptive mechanisms. J. Volcanol. Geotherm. Res., 17:273-288.

Rosi, M., Vezzoli, L., Aleotti, P. and De Censi, M., 1995. Interaction between caldera collapse and eruptive dynamics during the Campanian Ignimbrite eruption, Phlegraean Fields, Italy. Bull. Volcanol., 57: 541-554.

Scandone, R.M, Bellucci, F., Lirer, L. and Rolandi, G., 1991. The structure of the Campanian plain and the activity of the Neapolitan Volcanoes. J. Volcanol. Geotherm. Res., 48(1-2): 1-31.

Scarpati, C., Cole, P. and Perrotta, A., 1993. The Neapolitan Yellow Tuff - A large volume multiphase eruption from Campi Flegrei, Southern Italy. Bull. Volcanol., 55: 343-356.

Scherillo, A., 1953. Sulla revisione del foglio Napoli della Carta Geologica d'Italia. Boll. Serv. Geol. It., 75: 808-826.

Scherillo, A., 1955. Petrografia chimica dei tufi flegrei 2) tufo giallo, mappamonte, pozzolana. Rend. Acc. Sc. Fis. e Mat., 22: 317-330.

Scherillo, A. and Franco, E., 1960. Rilevamento stratigrafico del territorio comunale di Napoli. Boll. Soc. Natur., Napoli, 69: 255-262.

Scherillo, A. and Franco, E., 1967. Introduzione alla carta stratigrafica del suolo di Napoli. Atti Acc. Pontaniana, Napoli, 16: 27-37.

Smith, R.L., 1979. Ash-flow magmatism. Geol. Soc. Amer. Spec. Pap., 180: 5-27.

Smith, R.L. and Shaw, H.R., 1975. Igneous-related geothermal systems. In: D. E. White (Editor), Assessment of Geothermal Resources of the United States—1975. U. S. Geol. Surv. Circ. 726: 58-83.

Smith, R.L. and Shaw, H.R., 1979. Igneous-related geothermal systems. In: L.J.P. Muffler (Editor), Assessment of Geothermal Resources of the United States—1978. U. S. Geol. Surv. Circ. 790: 12-17.

Smith, R.L., Shaw, H.R., Luedke, R.G. and Russel, S.L., 1978. Comprehensive tables giving physical data and thermal energy estimates for young igneous systems in the United States. U. S. Geol. Surv. Open File Rep. 78-925.

Stimac, J., Goff, F. and Wohletz, K., 1997, Thermal modeling of the Clear Lake magmatic system, California: Implications for hot dry rock geothermal development. Los Alamos National Laboratory Report: LA-12778-MS, 38 pp.

Turcotte, D.L. and Schubert, G., 1982. Geodynamics, applications of continuum physics to geological problems. Wiley, New York, 450 pp.

Valentine, G.A., 1992. Magma chamber dynamics. In: Encyclopedia of Earth System Sciences, 3: 1-17.

Villemant, B.,1988. Trace element evolution in the Phlegraean Fields (Central Italy): fractional crystallization and selective enrichment. Contrib. Mineral. Petrol., 98: 169-183.

Wohletz, K. and Heiken, G., 1992. Volcanology and geothermal energy. University of California Press, Berkeley, California, 432 pp.

Wohletz, K., Orsi, G. and de Vita, S., 1995. Eruptive mechanisms of the Neapolitan Yellow Tuff interpreted from stratigraphic, chemical and granulometric data. J. Volc. Geotherm. Res., 67:263-290.

Zyvoloski, G., 1987. The effect of structural resurgence on the thermal evolution of the Creede caldera. Geol. Soc. Amer. Abstracts with Programs, 19: no.5.

Table 1. Summary of the basic models.

	Model 0	*Model 1*	*Model 1 Large*	*Model 2*	*Model 2 Large*	*Model 3*
Chamber shape	Cylindrical; top at 4 km	Cylindrical; top at 4 km	Cylindrical; top at 4 km	Cylindrical; top at 4 km	Cylindrical; top at 4 km	Cylindrical; top at 4 km
Chamber volume (km^3)	CI=1000 NYT=157	CI=1000 NYT=157	CI=2000 NYT=470	CI=1000 NYT=157	CI=2000 NYT=470	CI=1000 NYT=240
Injection history	None	CI: 37 ka	CI: 37 ka	CI: 37 ka	CI: 37 ka	CI: 200 (57 ka) 200 (52 ka) 200 (47 ka) 200 (42 ka) 200 (37 ka)
						NYT: 80 (28 ka) 80 (20 ka) 80 (12 ka)
		NYT: 12 ka	NYT: 12 ka	NYT: 12 ka	NYT: 12 ka	
		Minopoli: 0.4 km^3 at base of NYT	Minopoli: 0.4 km^3 at base of NYT	Minopoli: 0.4 km^3 at base of NYT	Minopoli: 0.4 km^3 at base of NYT	Minopoli: 0.4 km^3 at base of NYT
Volcanic structure	None	CI: 1 km collapse over 16 km diameter; NYT: 1 km collapse over 10 km	CI: 1 km collapse over 16 km diameter; NYT: 1 km collapse over 10 km	CI: 1 km collapse over 16 km diameter; NYT: 1 km collapse over 10 km	CI: 1 km collapse over 16 km diameter; NYT: 1 km collapse over 10 km	CI: 1 km collapse over 16 km diameter; NYT: 1 km collapse over 10 km
Cooling history	>600 ka	37 ka	37 ka	37 ka	37 ka	57 ka
Hydrothermal convection	None	Caldera: none;	Caldera: none;	Caldera: 1 km below CIc fill (37-0 ka); 0.5 km below NYTc fill (12-0 ka)	Caldera: 1 km below CIc fill (37-0 ka); 0.5 km below NYTc fill (12-4 ka)	Caldera: 1 km below CIc fill (37-4 ka); 0.5 km below NYTc fill (12-4 ka))
		Mofete fracture zone 1 km wide to 500 m depth (8-0 ka)	Mofete fracture zone 1 km wide to 500 m depth (8-0 ka)	Mofete fracture zone 1 km wide to 500 m depth (8-2 ka)	Mofete fracture zone 0.5 km wide to 2 km depth (8-2 ka)	Mofete fracture zone 0.5 km wide to 2 km depth (8-4 ka)
Thermal Difference at 2 km (°C)	L: -29 M: -122 SV: -109 (after ~ 360 ka)	L: -104 M: -233 SV: -202	L: -104 M: -233 SV: -202	L: -75 M: -27 SV: -62	L: -76 M: -25 SV: -65	L: -53 M: -12 SV: -27
Ave. T (°C)	634	858	870	858	870	844

Table 1. (Continued)

	Model 4	*Model 4a*	*Model 4b*	*Model 5*	*Model 5a*	*Model 6*
Chamber shape	Funnel, domed top; top at 4 km	Funnel, domed top; top at 4 km	Funnel, domed top; top at 3 km—collapse to 4 km	Funnel, flat top	Funnel, flat top	Spheroidal
Chamber volume (km^3)	CI=1000 NYT=240	CI=1000 NYT=240	CI=1000 NYT=240	CI=1000 NYT=240	CI=1000 NYT=240	CI=1754 NYT=240
Injection history (km^3)	CI: 140 (57 ka) 269 (52 ka) 240 (47 ka) 202 (42 ka) 150 (37 ka)	CI: 140 (87 ka) 269 (82 ka) 240 (77 ka) 202 (72 ka) 150 (67 ka) 140 (37 ka)	CI: 140 (57 ka) 269 (52 ka) 240 (47 ka) 202 (42 ka) 150 (37 ka)	CI: 284 (57 ka) 254 (52 ka) 231 (47 ka) 176 (42 ka) 55 (37 ka)	CI: 284 (57 ka) 254 (52 ka) 231 (47 ka) 176 (42 ka) 55 (37 ka)	CI: 250 (117 ka) 382 (97 ka) 314 (77 ka) 411 (57 ka) 397 (37 ka)
	NYT: 80 (28 ka) 80 (20 ka) 80 (12 ka)	NYT: 80 (28 ka) 80 (20 ka) 80 (12 ka)	NYT: 80 (28 ka) 80 (20 ka) 80 (12 ka)	NYT: 80 (28 ka) 80 (20 ka) 80 (12 ka)	NYT: 80 (28 ka) 80 (20 ka) 80 (12 ka)	NYT: 80 (28 ka) 80 (20 ka) 80 (12 ka)
	Minopoli: 0.4 km^3 at base of NYT	Minopoli: 0.4 km^3 at base of NYT	Minopoli: 0.4 km^3 at base of NYT	Minopoli: 0.4 km^3 at base of NYT	Minopoli: 40 km^3 at base of NYT	Minopoli: 1 km^3 at base of NYT
Volcanic structure	CI: 1 km collapse over 16 km diameter; NYT: 1 km collapse over 10 km	CI: 1 km collapse over 16 km diameter; NYT: 1 km collapse over 10 km	CI: 1 km collapse over 16 km diameter; NYT: 1 km collapse over 10 km	CI: 1 km collapse over 16 km diameter; NYT: 1 km collapse over 10 km	CI: 1 km collapse over 16 km diameter; NYT: 1 km collapse over 10 km	CI: 1 km collapse over 16 km diameter; NYT: 1 km collapse over 10 km
Cooling history	57 ka	87 ka	57 ka	57 ka	57 ka	117 ka
Hydrothermal convection	Caldera: 1 km below CIc fill (37-4 ka); 0.5 km below NYTc fill (12-4 ka)	Caldera: 1 km below CIc fill (37-4 ka); 0.5 km below NYTc fill (12-4 ka)	Caldera: 1 km below CIc fill (37-4 ka); 0.5 km below NYTc fill (12-4 ka)	Caldera: 1 km below CIc fill (37-4 ka); 0.5 km below NYTc fill (12-4 ka)	Caldera: 1 km below CIc fill (37-4 ka); 0.5 km below NYTc fill (12-4 ka)	Caldera: 1 km below CIc fill (37-4 ka); 0.5 km below NYTc fill (12-4 ka)
	Mofete fracture zone 0.5 km wide to 2 km depth (8-4 ka)	Mofete fracture zone 0.5 km wide to 2 km depth (8-4 ka)	Mofete fracture zone 0.5 km wide to 2 km depth (8-4 ka)	Mofete fracture zone 0.5 km wide to 2 km depth (8-4 ka)	Mofete fracture zone 0.5 km wide to 2 km depth (8-4 ka)	Mofete fracture zone 0.5 km wide to 2 km depth (8-4 ka)
Thermal Difference at 2 km (°C)	L: -79 M: +4 SV: -64	L: -55 M: +40 SV: -1	L: -37 M: +90 SV: +55	L: -23 M: +13 SV: -25	L: -22 M: +13 SV: +23	L: -76 M: +5 SV: -35
Ave. T (°C)	844	854	843	850	842	

Figures
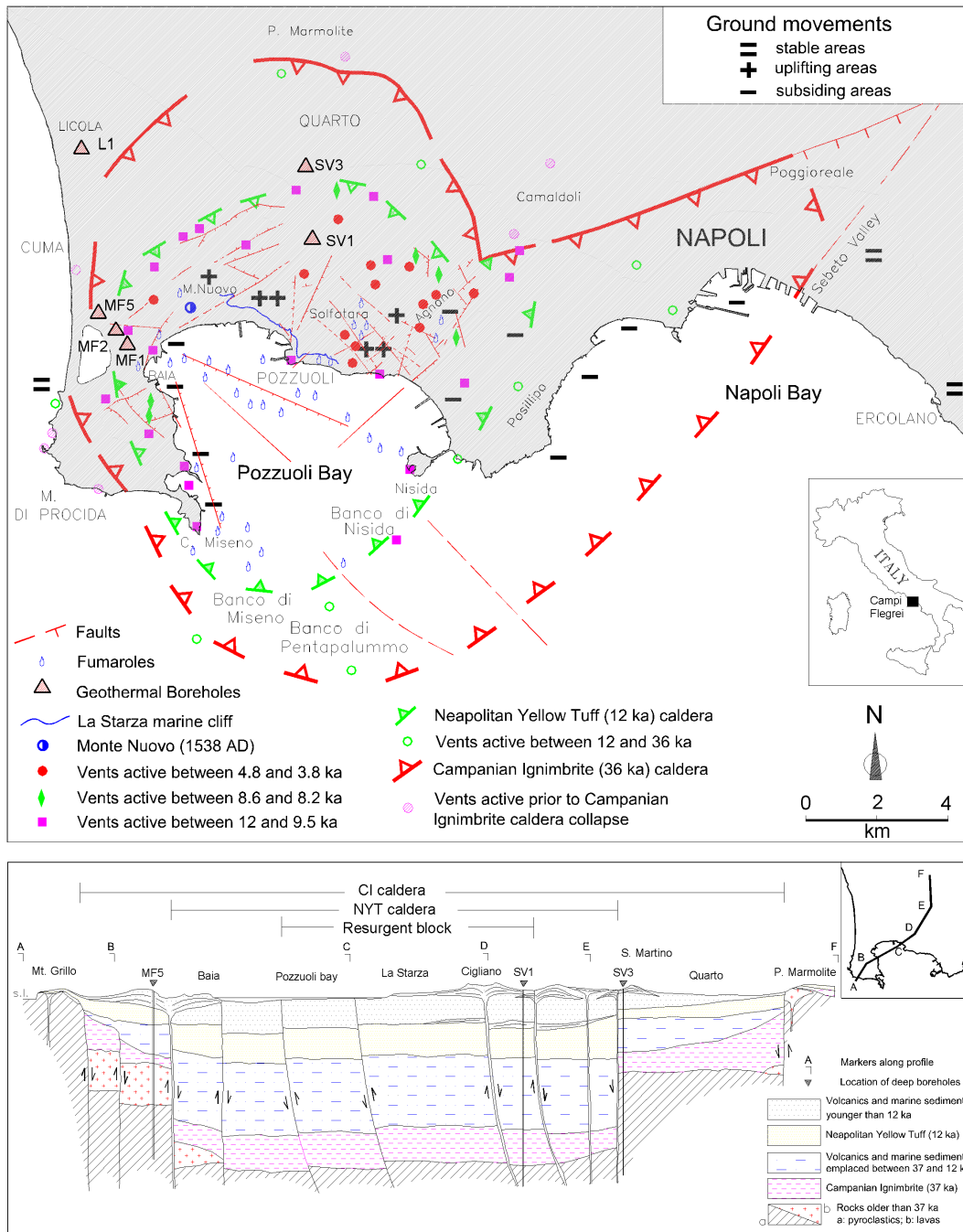
Fig. 1. Geological map and cross section of the Campi Flegrei caldera. The map depicts the basic structural elements of the caldera, the locations of recent vents and geothermal manifestations, and the locations of geothermal boreholes where thermal gradients have been measured.
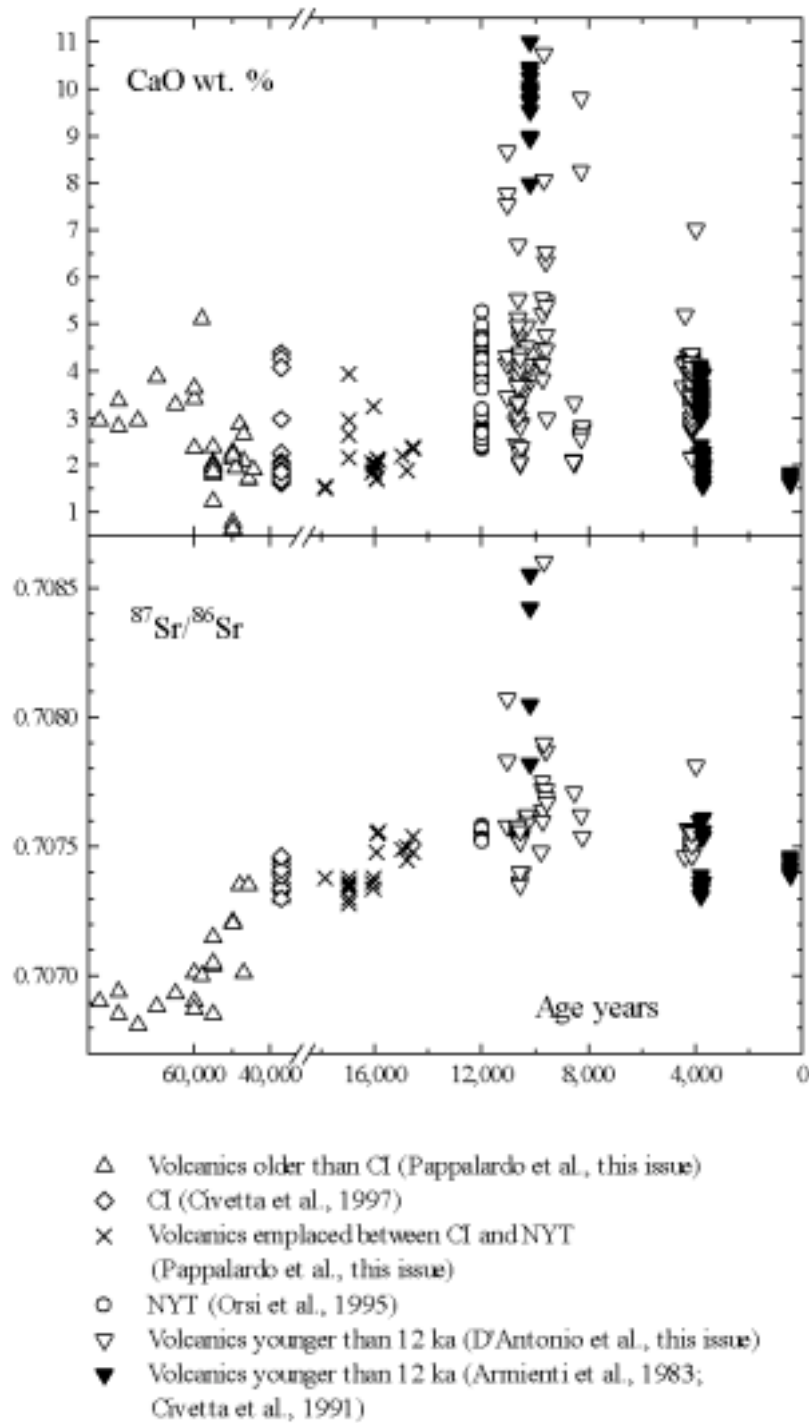
Fig. 2. Geochemical trends of extruded Phlegraean magmas are shown as CaO abundances and ^{87}Sr/^{86}Sr ratios from ~60 ka bp to present. The diamonds indicate the major extrusion of the Campanian ignimbrite and the circles indicate the Neapolitan Yellow Tuff extrusion.
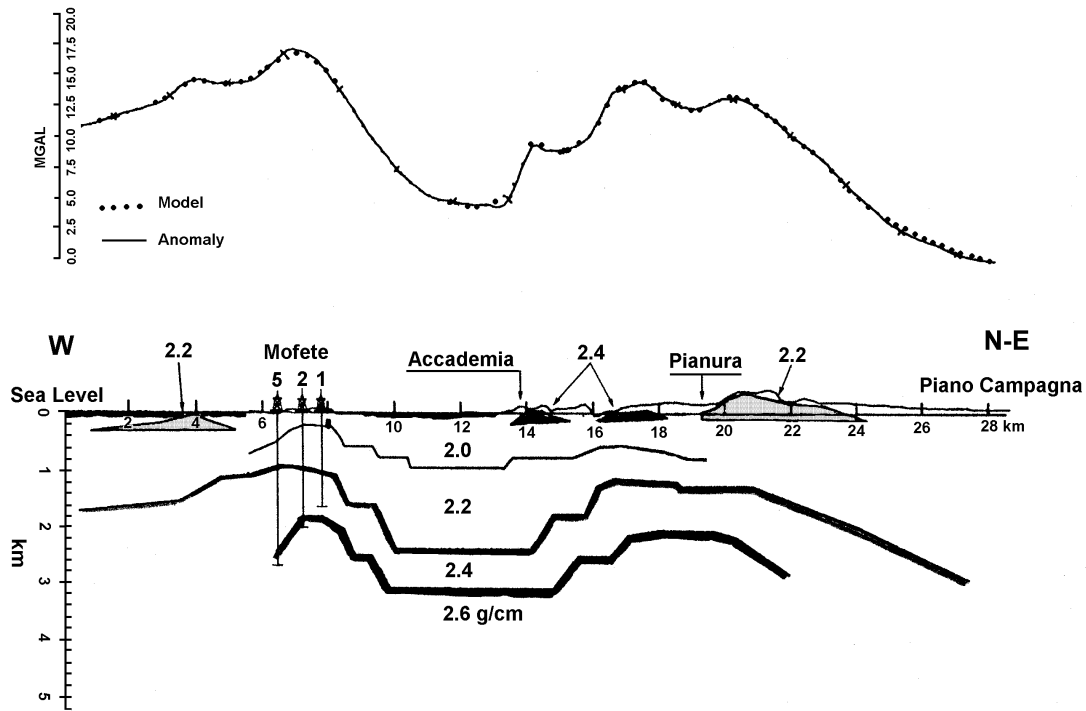
Fig. 3. A W-NE Gravimetric profile from AGIP (1987), showing the 2-D density model fit to the profile. The density structure shows the western and northeastern caldera margins of the caldera where less dense rocks project to relatively greater depths.
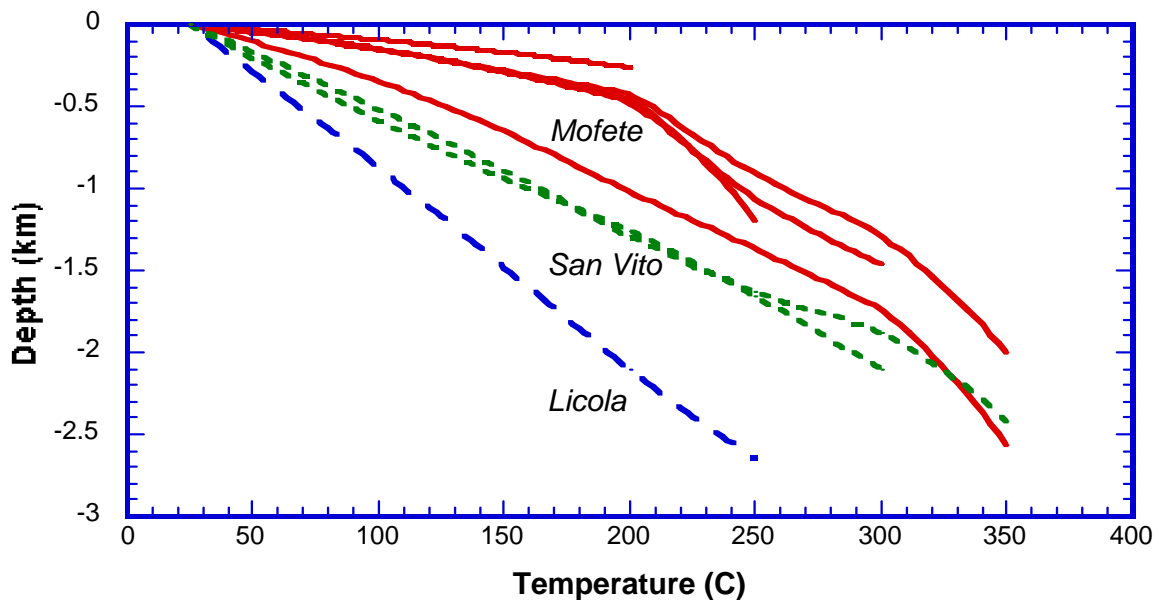
Fig. 4. Geothermal gradients (AGIP, 1987). While those gradients measured at Mofete (solid) show an abrupt steepening at a depth of about ~0.5 km characteristic of hydrothermal convection, this feature is shown by only one of the gradients at San Vito (dotted) and is absent for the profile at Licola (dashed).
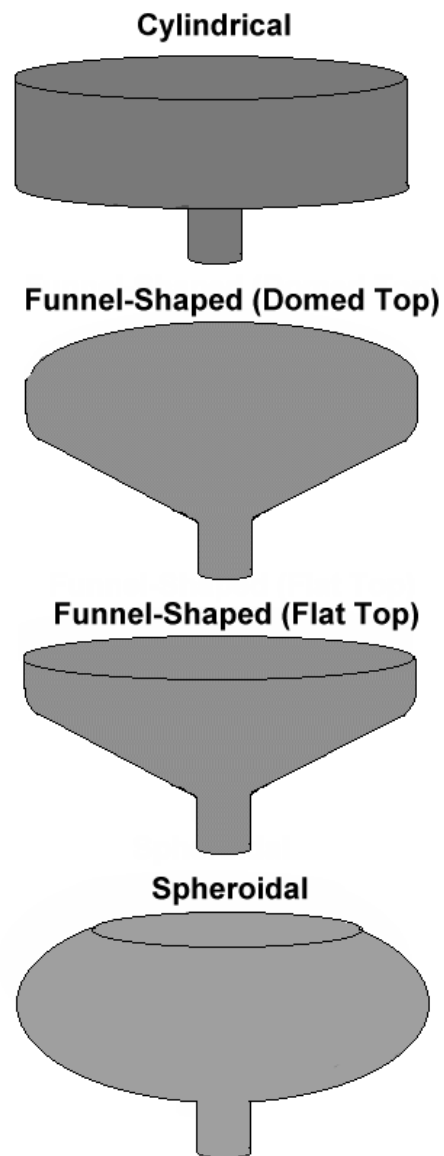
Fig. 5. Sketch illustrations of 4 principal magma chamber shapes modeled.
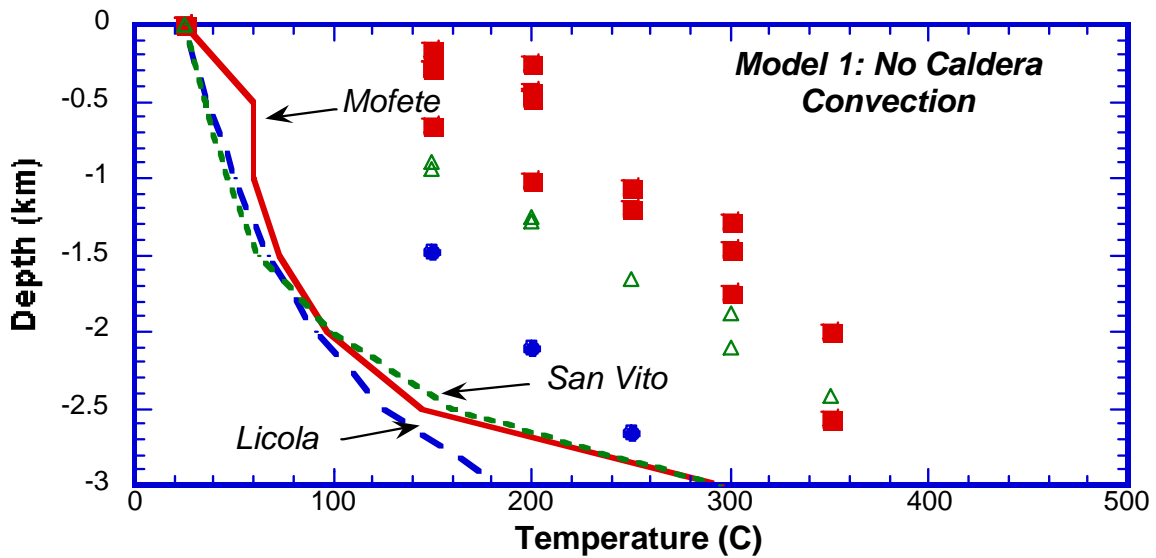
Fig. 6. Model 1 results show that computed conductive thermal gradients are much lower than those measured, suggesting for this set of boundary conditions that hydrothermal convection is required to bring more heat to surface rocks within the time frame of the model. The symbols used in this plot and following plots are Licola (solid circles and dashed curve), San Vito (open triangles and dotted curve), and Mofete (solid squares and solid curve).
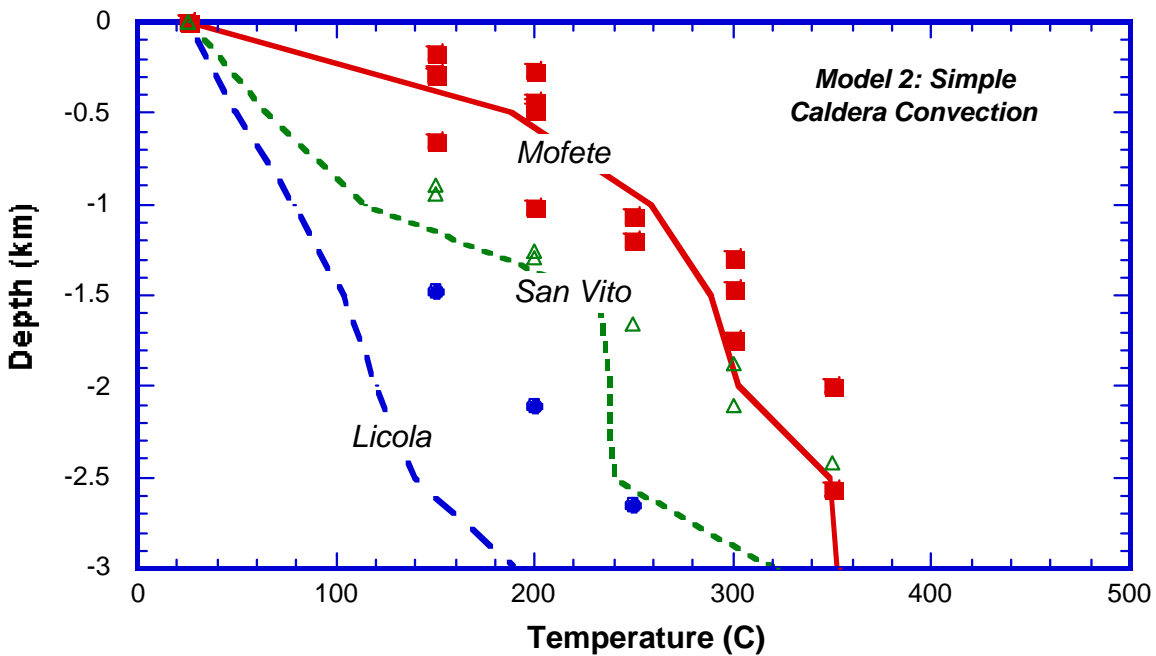
Fig. 7. Model 2 shows the pronounced affects of hydrothermal convection within rocks below the caldera and above the modeled magma chamber. Still, Licola, situated outside the caldera margin where convection does not play a role shows too little heat flow.
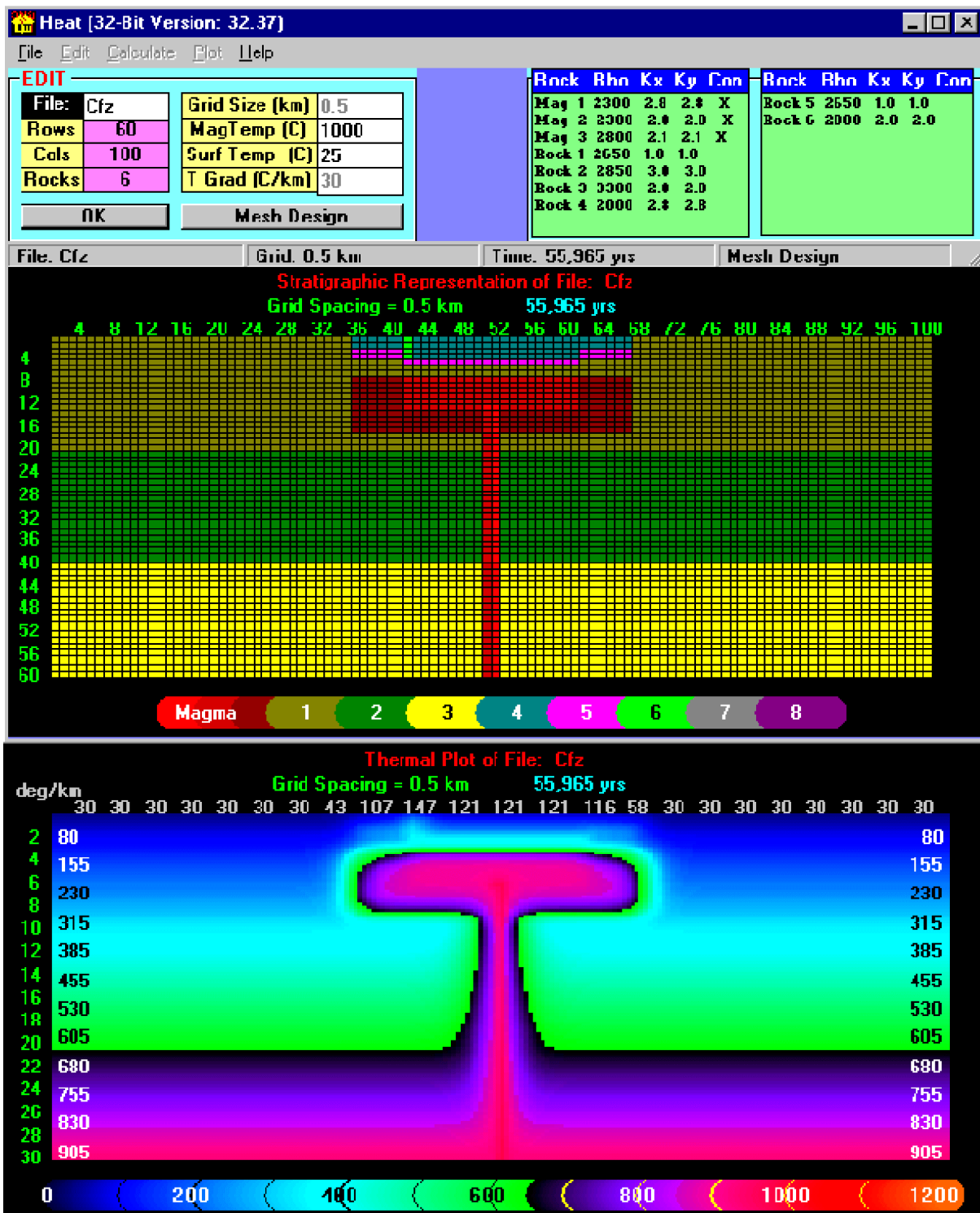
Fig. 8. Numerical mesh (top) and thermal plot (bottom), showing west to east profiles of Model 3. The mesh shows the simple cylindrical magma chamber shape and stratigraphic sequence as cells of different colors (note the caldera fill rocks of teal and magenta defining the margins of the Campanian outer and NYT (inner) calderas). Isotherms, represented by changes in color, bend upward above the magma chamber significantly raised in the Mofete area near the western margin of the caldera.
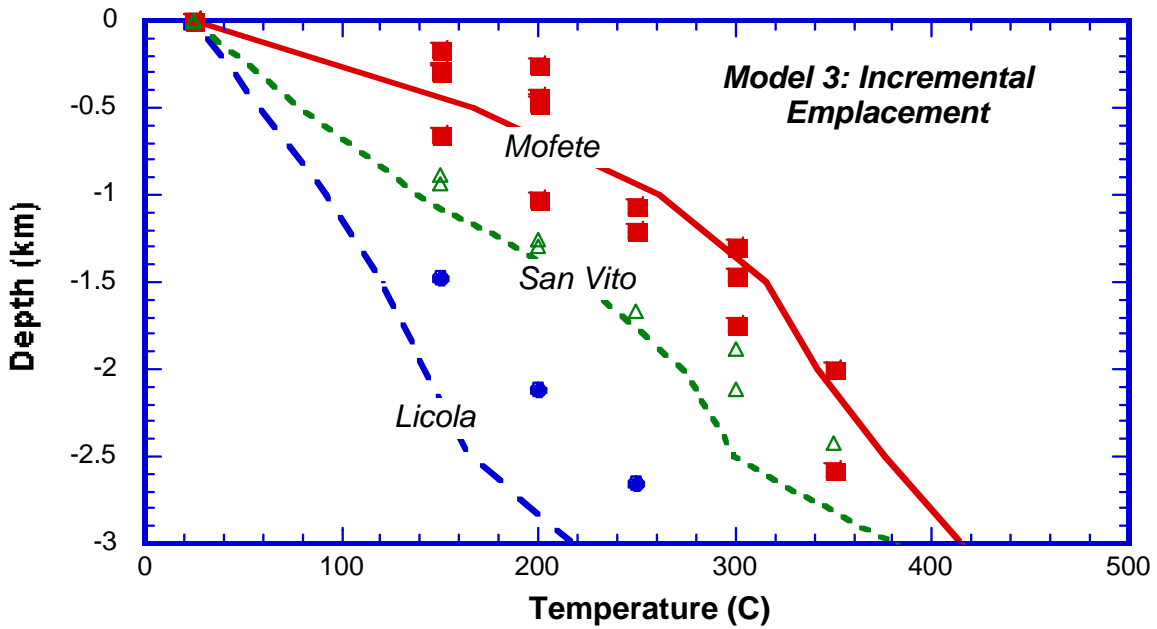
Fig. 9. Model 3 thermal gradients are adequate fits to measured data with the exception of the gradient at Licola, which is too low.
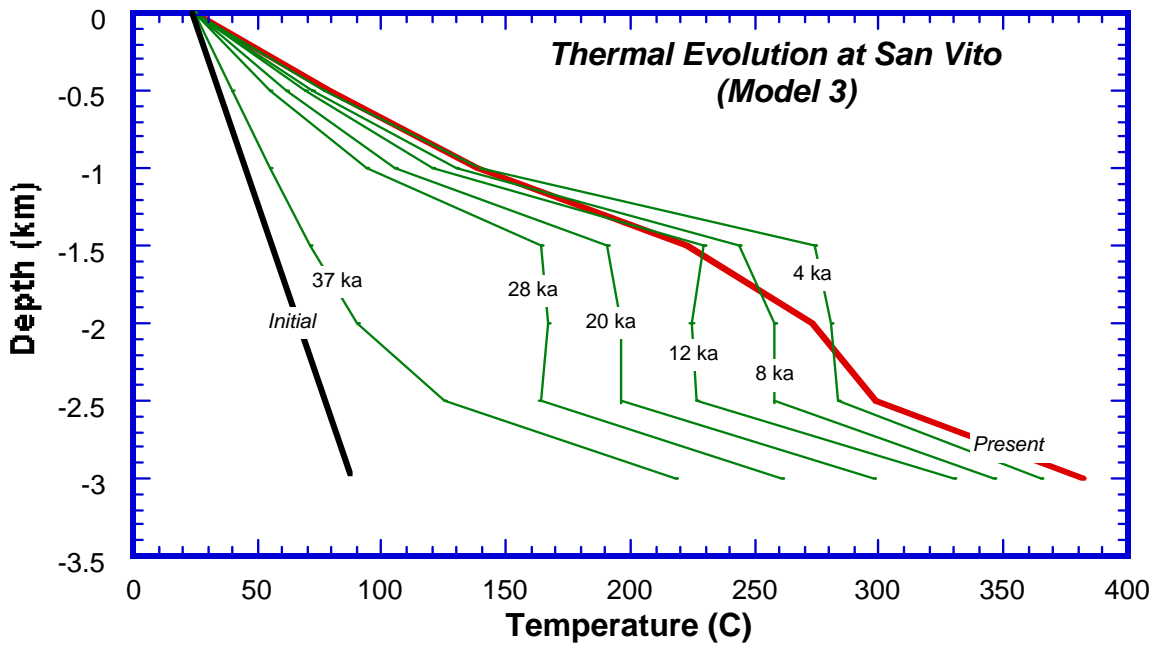
Fig. 10. Model 3 thermal evolution shows computed thermal gradients at San Vito from initial conditions at 50 ka bp to the present. Steep gradient from 28 ka to 4 ka are the result of caldera convection.
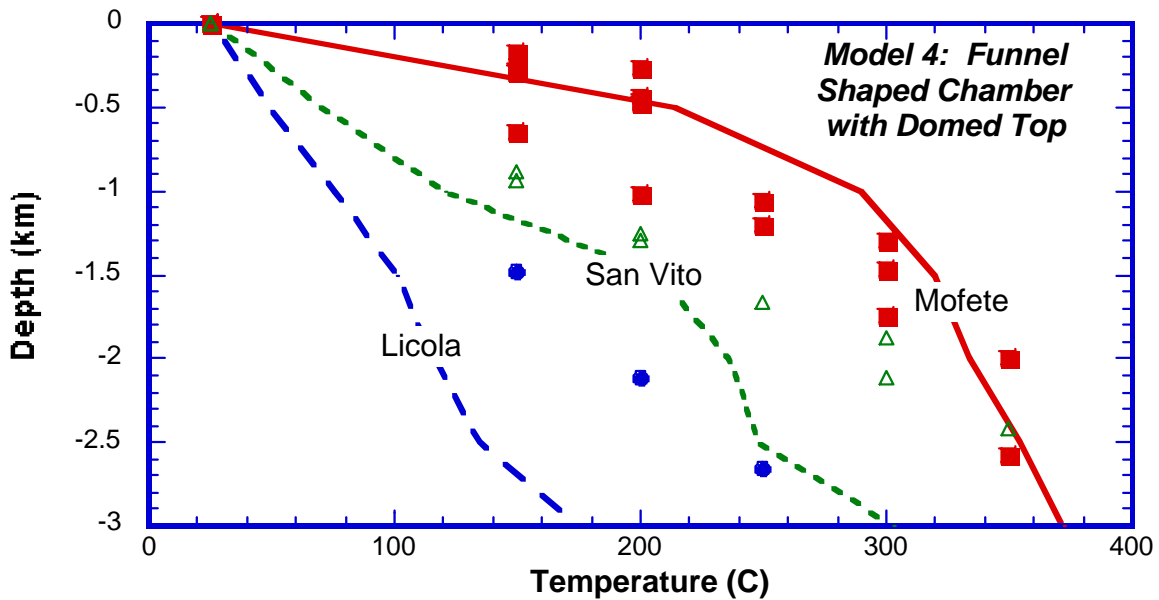
Fig. 11. Model 4 gradients show that the domed top of the magma chamber concentrates more heat near the center of the caldera but does not provide enough around its margins (Licola).
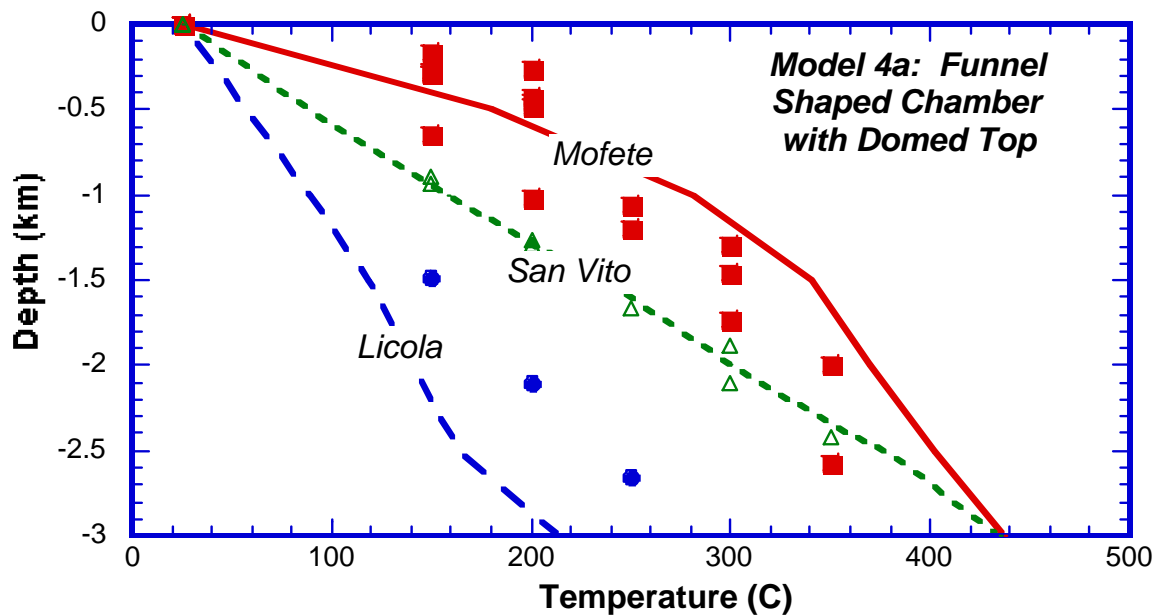
Fig. 12. Model 4a gradients result from starting magma chamber growth 50 ka before eruption of the Campanian ignimbrite, which helps to make San Vito gradients acceptable but does not help at Licola.
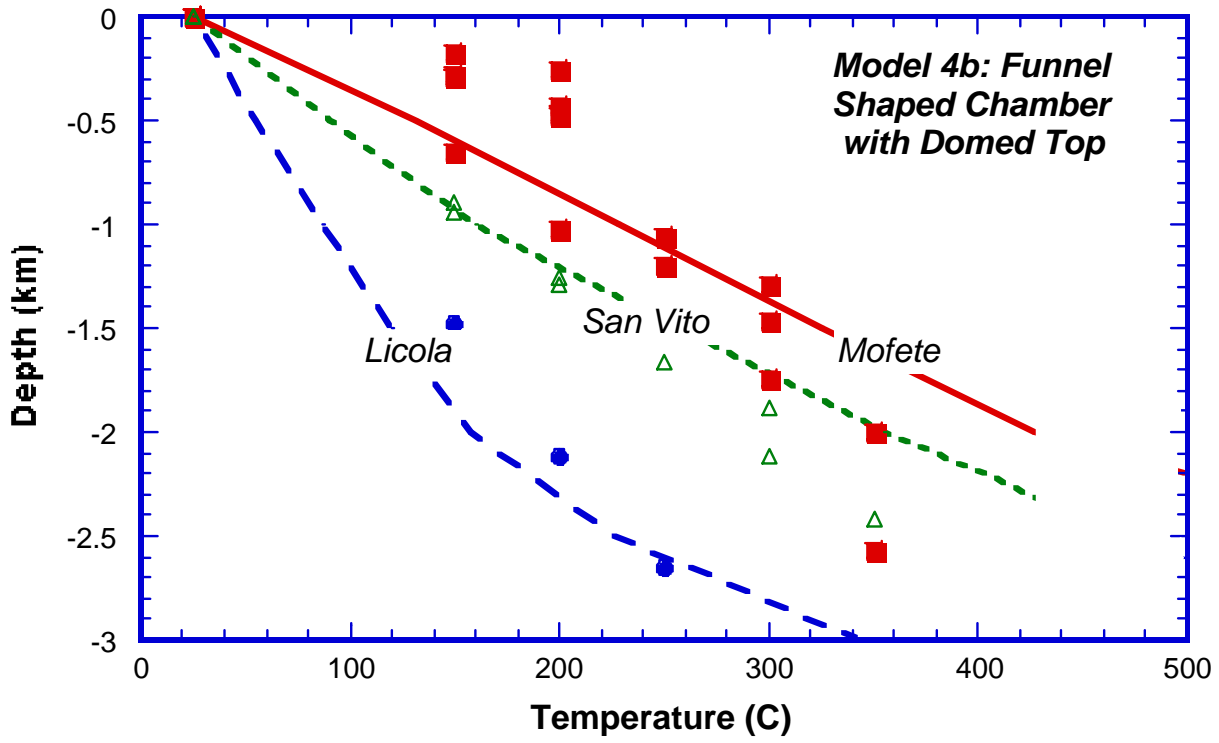
Fig. 13. Model 4b gradients result from placing the domed top at 3 km depth, which helps to match the Licola gradient but makes the San Vito gradient too high.
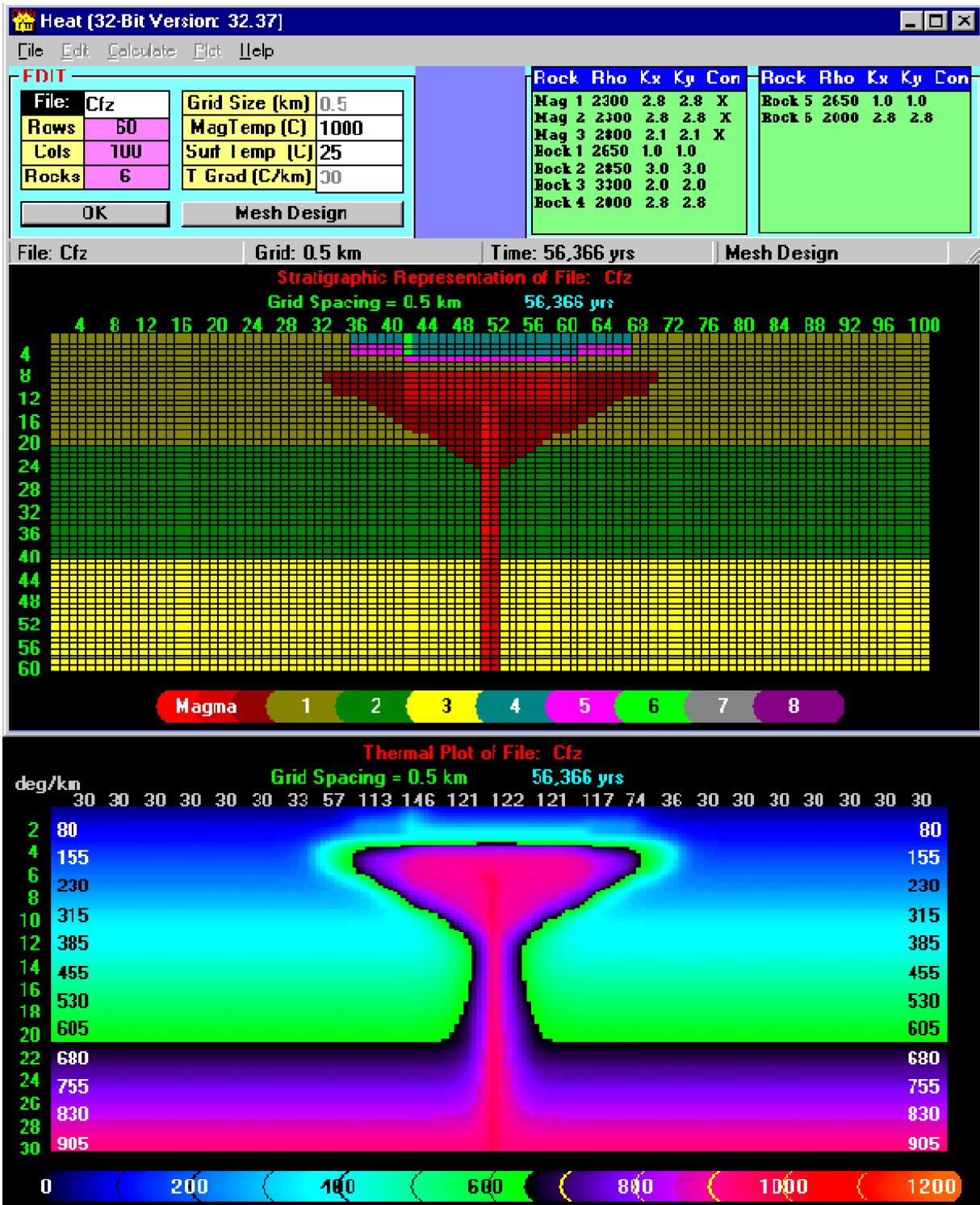
Fig. 14. Model 5 mesh and thermal plot for a funnel-shaped chamber with a flat top. This chamber shape helps spread heat to the caldera margin localities.
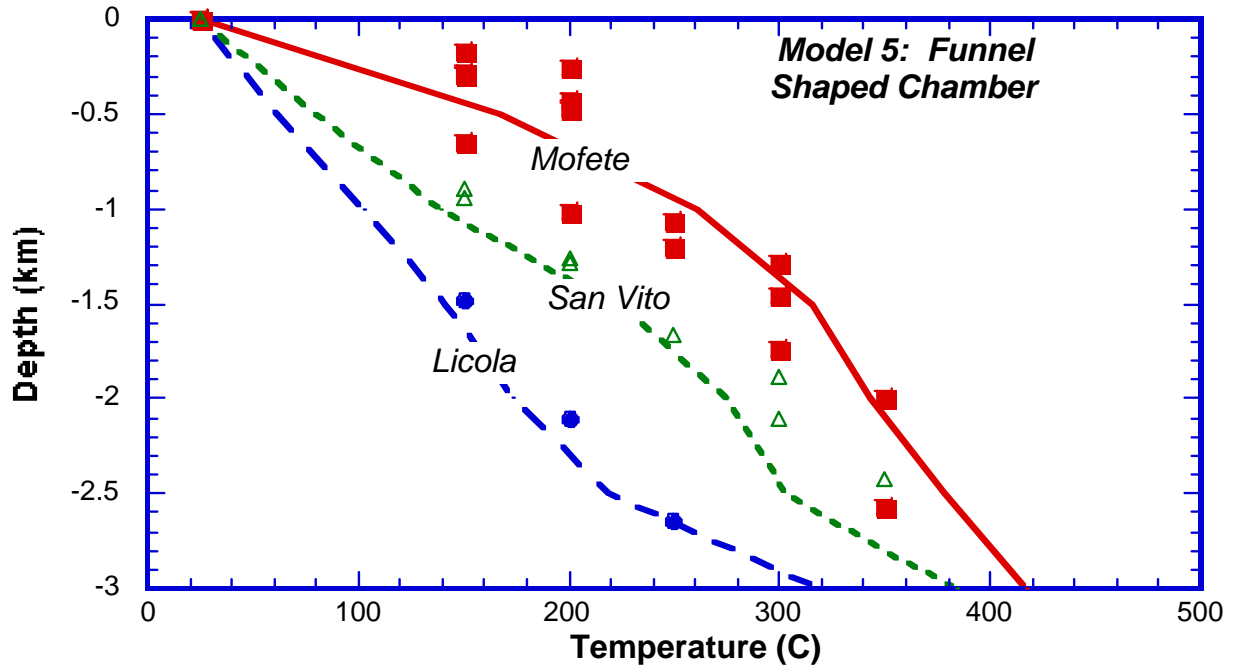
Fig. 15. Model 5 thermal gradients show acceptable results for all localities produced by a funnel-shaped chamber with a flat top.
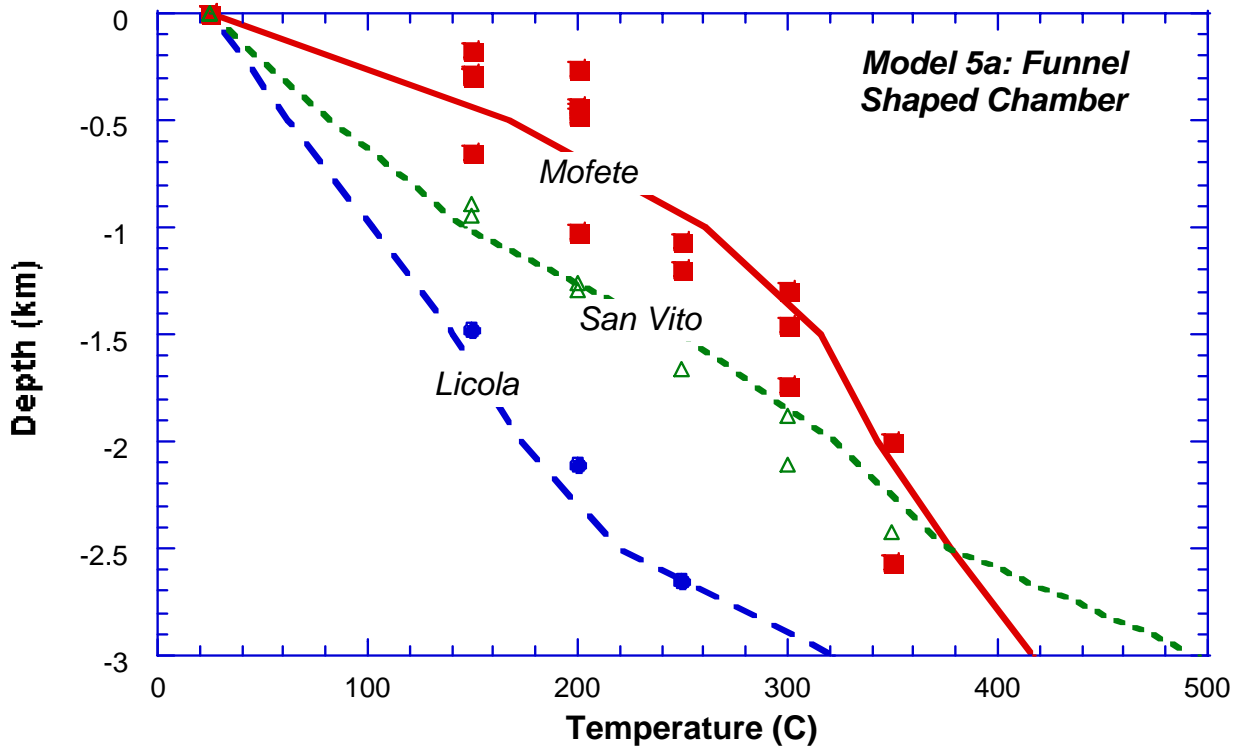
Fig. 16. Model 5a thermal gradients show perhaps an improvement of the San Vito model, which results from a dike-like intrusion along the caldera margin near San Vito.
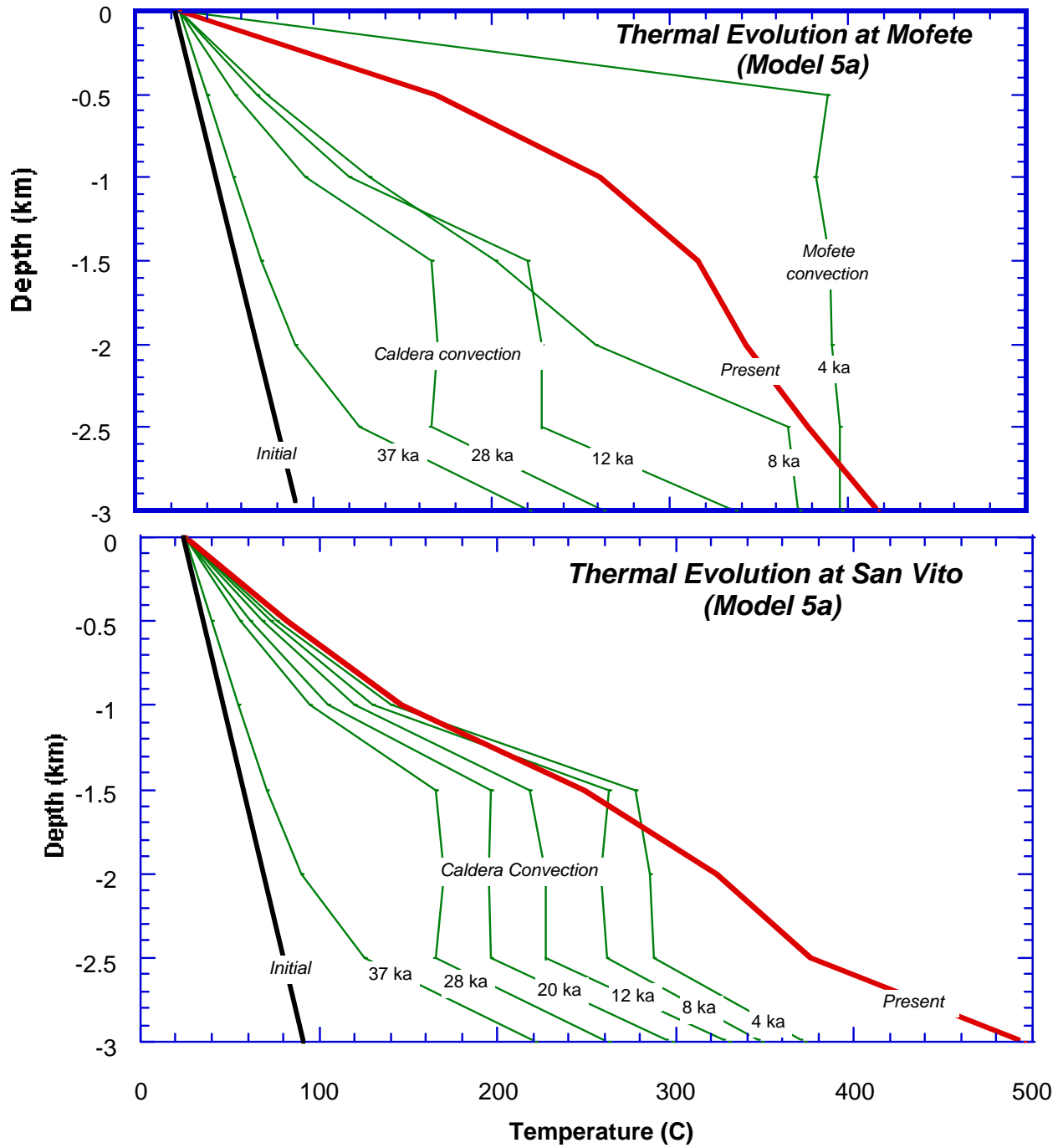
Fig. 17. Model 5a thermal gradient evolution at Mofete and San Vito. Note that at the end of convection at Mofete (4 ka), the thermal gradient is very high after which it relaxes to present day conditions.
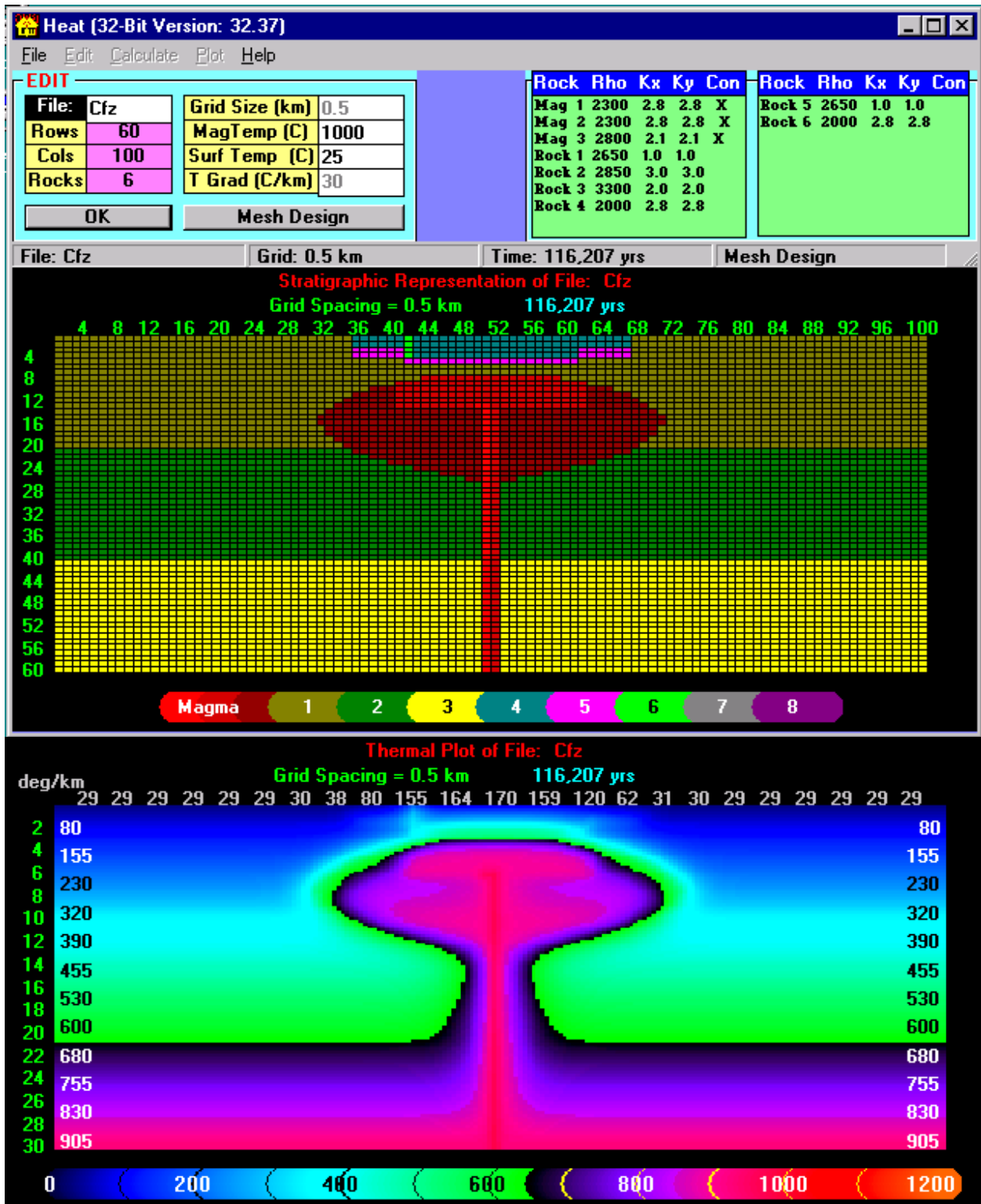
Fig. 18. Model 6 mesh and thermal plot illustrates that a very large volume is required for a spheroidal chamber shape to get enough heat to the surface over the lifetime of the system.
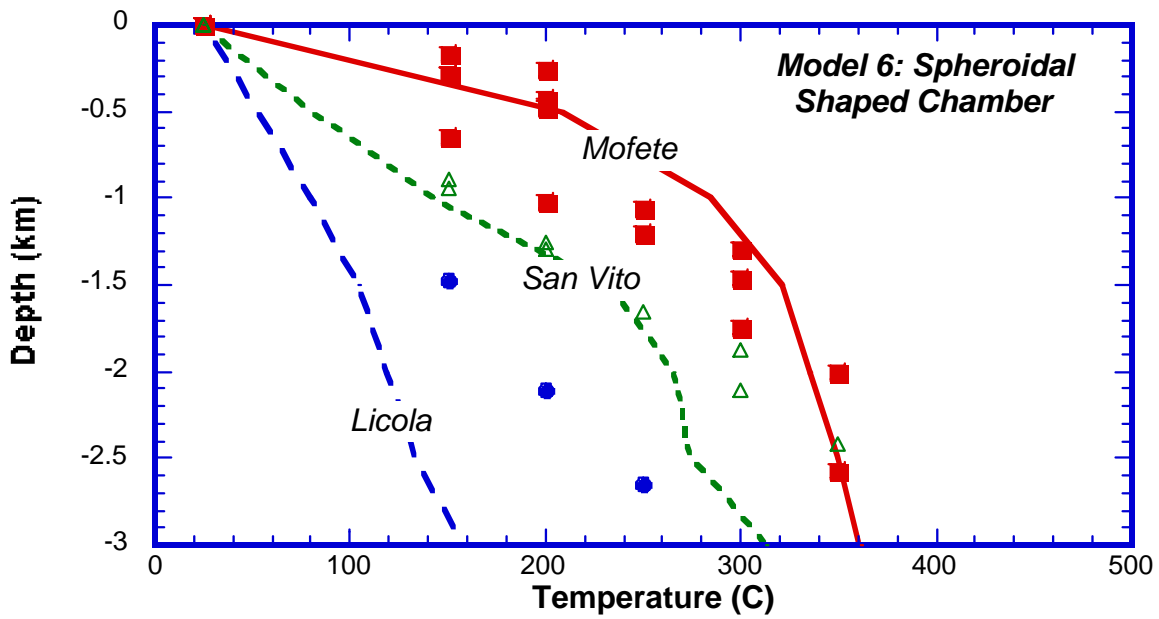
Fig. 19. Model 6 thermal gradients are adequate for all but Licola, which just does not "feel" enough heat from the magma chamber margins, which are at a relatively great depth for this spheroidal chamber.
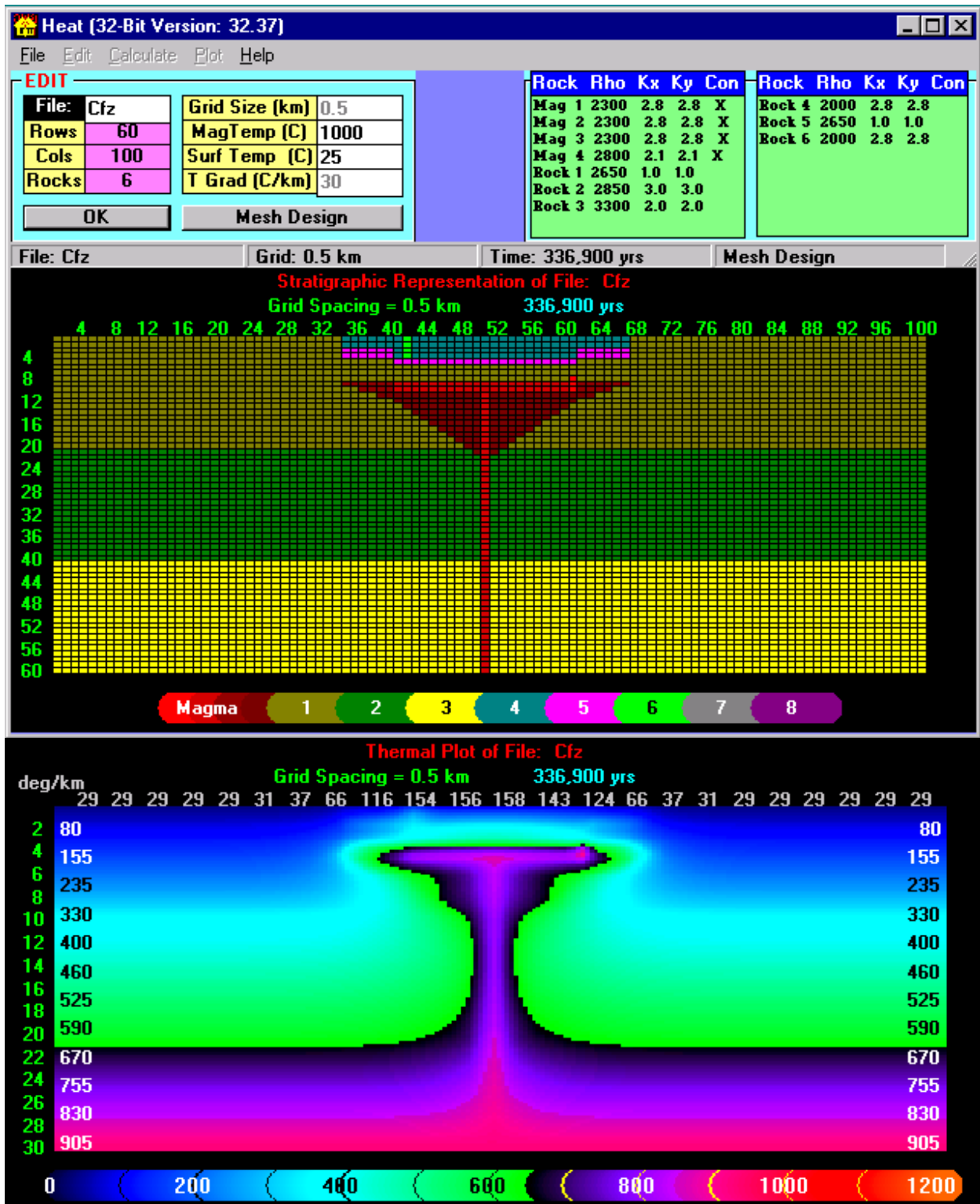
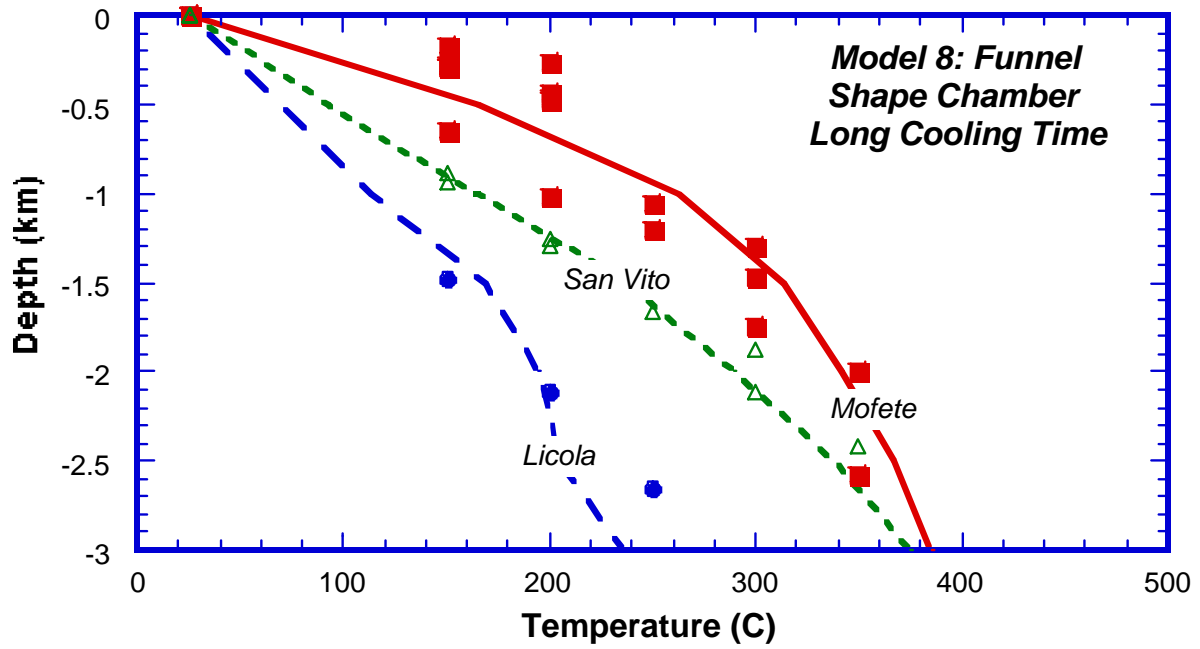Fig. 20.   Model 8 mesh and thermal plot illustrating the funnel-shaped chamber, which develops over 300 ka.

Fig. 21. Model 8 thermal gradients show good representations of measured data with a slight deviation at depth for Licola.